Characterization of chronic aortic and mitral regurgitation using echocardiography and cardiovascular magnetic resonance

Christian Lars Polte

Department of Molecular and Clinical Medicine
Institute of Medicine
Sahlgrenska Academy at the University of Gothenburg

UNIVERSITY OF GOTHENBURG

Gothenburg 2015

Cover illustration: Linear and volumetric multimodality phantom model as well as imaging of aortic and mitral regurgitation using color Doppler echocardiography and cardiovascular magnetic resonance by Christian Lars Polte

Characterization of chronic aortic and mitral regurgitation using echocardiography and cardiovascular magnetic resonance

christian.polte@vgregion.se

ISBN 978-91-628-9467-2 (Printed edition)
ISBN 978-91-628-9468-9 (Electronic edition)
E-publication: http://hdl.handle.net/2077/38759

Printed in Gothenburg, Sweden 2015
by Ineko AB

“Science is not only a disciple of reason but,
also, one of romance and passion.”

Stephen Hawking

This thesis is dedicated **to my family** who has provided immense support and encouragement throughout my career.

Characterization of chronic aortic and mitral regurgitation using echocardiography and cardiovascular magnetic resonance

Christian Lars Polte

Department of Molecular and Clinical Medicine, Institute of Medicine,
Sahlgrenska Academy at the University of Gothenburg
Gothenburg, Sweden

ABSTRACT

Introduction
Grading of chronic aortic (AR) and mitral regurgitation (MR) severity can be obtained by echocardiography and cardiovascular magnetic resonance (CMR). The aims of the four studies were: (1) to establish echocardiographic thresholds for left ventricular (LV) dimensions indicating severe chronic AR or MR, using CMR as reference, (2) to elucidate the main cause of echocardiographic underestimation of LV dimensions compared with CMR, (3) to systematically compare three indirect CMR MR quantification methods ('standard', 'volumetric' and 'flow' method), as well as (4) to establish CMR- and quantification method-specific thresholds indicating hemodynamically significant chronic AR or MR benefiting from surgery.

Methods
The first prospective study comprised a total of 93 (AR (n=44), MR (n=49)), the second 45 (healthy volunteers (n=20), AR (n=17), MR (n=8)), the third 52 (healthy volunteers (n=16), MR (n=36)) and the fourth 78 participants (AR (n=38), MR (n=40)). Two-dimensional (2DE) and real-time three-dimensional echocardiography (RT3DE) as well as CMR was performed in all participants. Operated patients with severe AR/MR, according to 2DE, underwent also post-surgical scans. Furthermore, a multimodality phantom model was investigated.

Results
(1) Linear dimensions could not sufficiently identify severe LV dilatation, in contrast to 2DE volumes, which showed an excellent (AR) or good (MR) diagnostic ability. The diagnostic ability was less powerful for RT3DE volumes. (2) All modalities delineated the phantom model with high precision. *In vivo*, 2DE/RT3DE under-

estimated LV short-axis end-diastolic linear, areal and all volumetric dimensions significantly compared with CMR, but not short-axis end-systolic linear and areal dimensions. (3) The 'standard' method determined significantly larger regurgitant volumes (RV) and fractions (RF), in contrast to the 'volumetric' and 'flow' method, which determined similar results. This affected the grading of severity in operated MR patients. (4) In operated patients, application of current RF thresholds by CMR led to frequent downgrading compared with 2DE. Furthermore, CMR- and quantification method-specific thresholds were established, which were lower than recognized guideline criteria.

Conclusions
(1) LV volumes obtained by 2DE/RT3DE can support the diagnosis of severe AR and MR, when other causes of LV dilation have been considered. (2) Echocardiographic underestimation of LV dimensions is mainly due to inherent technical differences in the ability to differentiate trabeculated from compact myocardium. (3) The choice of indirect CMR MR quantification method can affect the grading of regurgitation severity and thereby eventually the clinical decision-making. (4) CMR grading of chronic AR and MR severity should be based on modality- and quantification method-specific thresholds to assure appropriate clinical decision-making.

Keywords
Aortic regurgitation • Mitral regurgitation • Grading of severity • Left ventricular dimensions • Echocardiography • Cardiovascular magnetic resonance

ISBN 978-91-628-9467-2 (Printed edition)
ISBN 978-91-628-9468-9 (Electronic edition)
E-publication: http://hdl.handle.net/2077/38759

SAMMANFATTNING PÅ SVENSKA

Introduktion

Indelning av kronisk aorta- (AI) och mitralisinsufficiens (MI) i olika svårighetsgrader kan genomföras med hjälp av ekokardiografi och kardiovaskulär magnetresonans (KMR). Syftet med de fyra studierna var: (1) att etablera ekokardiografiska tröskelvärden för vänsterkammardimensioner som indikerar stor AI eller MI med KMR som referens, (2) att belysa huvudorsaken för den ekokardiografiska underskattningen av vänsterkammardimensioner jämfört med KMR, (3) att jämföra tre indirekta KMR metoder för kvantifiering av MI ('standard', 'volymetrisk' och 'flödes' metod), och (4) att etablera KMR- och kvantifieringsmetodspecifika tröskelvärden som indikerar hemodynamisk betydande AI eller MI som har nytta av kirurgi.

Metoder

Första prospektiva studien omfattar 93 (AI (n=44), MI (n=49)), andra studien 45 (friska frivilliga (n=20), AI (n=17), MI (n=8)), tredje studien 52 (friska frivilliga (n=16), MI (n=36)) och fjärde studien 78 deltagare (AI (n=38), MI (n=40)). Tvådimensionell (2DE) och tredimensionell ekokardiografi (3DE) samt KMR genomfördes på alla deltagare. Opererade patienter med stor AI/MI, enligt 2DE, genomgick också undersökningar efter kirurgi. Dessutom undersöktes en multimodal fantom modell.

Resultat

(1) Lineära dimensioner kunde inte identifiera betydande vänsterkammardilatation i tillräkligt utsträckning, däremot visade 2DE

volymer excellent (AI) eller bra (MI) diagnostisk förmåga. Den diagnostiska förmågan var sämre för 3DE. (2) Alla modaliteter kunde avbilda fantomdimensionerna med hög precision. *In vivo* underskattade 2DE/3DE vänsterkammarens slutdiastoliska diameter och area i kortaxel och alla volymer, men inte den slutsystoliska diameter och area i kortaxel. (3) 'Standard' metoden kvantifierade signifikant större regurgitationsvolymer (RV) och fraktioner (RF) jämförd med 'volymetrisk' och 'flödes' metod, som kom fram till liknande resultat. Skillnaden mellan metoderna påverkade graderingen av svårighetsgraden i opererade patienter. (4) Tillämpning av RF tröskelvärden enligt de aktuella behandlings-riktlinjerna gällande KMR ledde i opererade patienter ofta till nedgradering jämfört med 2DE. Dessutom etablerades KMR- och kvantifieringsmetodspecifika tröskelvärden, som var lägre än de aktuella tröskelvärdena från behandlingsriktlinjerna.

Slutsatser

(1) 2DE/3DE vänsterkammarvolymer kan stödja diagnosen av stor AI och MI, när andra orsaker för kammardilatation har övervägts. (2) Ekokardiografisk underskattning av vänsterkammardimensionerna orsakas huvudsakligen av tekniska skillnader i förmågan att skilja trabekulerad från kompakt myokard. (3) Val av indirekt KMR kvantifieringsmetod gällande MI kan påverka gradering och därmed eventuellt kliniskt beslutsfattande. (4) KMR gradering av kronisk AI och MI bör baseras på modalitets- och kvantifieringsmetodspecifika tröskelvärden för att säkerställa ett korrekt kliniskt beslutsfattande.

LIST OF PAPERS

This thesis is based on the following studies, referred to in the text by their Roman numerals:

I. *Left ventricular volumes by echocardiography can support the diagnosis of severe chronic aortic and mitral regurgitation: a prospective study using cardiovascular magnetic resonance as reference*

Bech-Hanssen O, Polte CL, Lagerstrand KM, Johnsson ÅA, Fadel BM and Gao SA

Submitted manuscript

II. *Quantification of left ventricular linear, areal and volumetric dimensions: a phantom and in vivo comparison of 2D and real-time 3D echocardiography with cardiovascular magnetic resonance*

Polte CL, Lagerstrand KM, Gao SA, Lamm CR and Bech-Hanssen O

Ultrasound Med Biol. 2015; 41 (7): 1981-1990
doi: 10.1016/j.ultrasmedbio.2015.03.001

III. *Mitral regurgitation quantification by cardiovascular magnetic resonance: a comparison of indirect quantification methods*

Polte CL, Bech-Hanssen O, Johnsson ÅA, Gao SA and Lagerstrand KM

Int J Cardiovasc Imaging. 2015; 31 (6): 1223-1231
doi: 10.1007/s10554-015-0681-3

IV. *Characterization of chronic aortic and mitral regurgitation benefiting from valve surgery using cardiovascular magnetic resonance*

Polte CL, Gao SA, Johnsson ÅA, Lagerstrand KM and Bech-Hanssen O

Submitted manuscript

CONTENT

ABBREVIATIONS

AoFF	Aortic forward flow
AR	Aortic regurgitation
BPE	Background phase error
CMR	Cardiovascular magnetic resonance
ECG	Electrocardiography
EDA	End-diastolic area
EDD	End-diastolic diameter
EDV	End-diastolic volume
EF	Ejection fraction
ESA	End-systolic area
ESD	End-systolic diameter
ESV	End-systolic volume
LA	Long-axis
LAA	Left atrial area
LoA	Limits of agreement
LV	Left ventricular
LVEF	Left ventricular ejection fraction
LVSV	Left ventricular stroke volume
MD	Mean difference
MiIF	Mitral inflow
MR	Mitral regurgitation
NLR	Negative likelihood ratio
PC	Phase-contrast velocity

PLA	Parasternal long-axis
PLR	Positive likelihood ratio
PuSV	Pulmonary stroke volume
RF	Regurgitant fraction
ROC	Receiver operating characteristics curve
ROI	Region of interest
RT3DE	Real-time three-dimensional echocardiography
RV	Regurgitant volume
RVSV	Right ventricular stroke volume
SA	Short-axis
SD	Standard deviation
SV	Stroke volume
VENC	Velocity encoding range
VHD	Valvular heart disease
2DE	Two-dimensional echocardiography
4CH	Four-chamber

1 INTRODUCTION

Valvular heart disease (VHD), although not as common as coronary artery disease or heart failure, is an important clinical entity, which is expected to increase in prevalence with the aging population (1-3). Over the past decades, important changes have occurred in Western countries concerning the distribution of patient characteristics and etiologies. These changes are characterized by a continuous increase in the incidence of degenerative valve disease due to an aging population and a simultaneous successive decline in rheumatic valve disease due to improved living conditions and health care (4). The increase in the proportion of elderly patients poses also additional challenges for the clinical management and leads to a higher intervention risk, as multiple co-morbidities are a frequent finding in this patient population (1,2). While few changes have occurred concerning the medical therapy of VHD, new surgical interventions and more recently transcatheter interventions have led to a shift in the overall treatment paradigms (5,6). Furthermore, early surgery in asymptomatic patients has been advocated (5-10). To assure appropriate clinical decision-making and timing of intervention, accurate assessment of disease severity is imperative, which is nowadays mainly based on non-invasive imaging techniques such as echocardiography and/or cardiovascular magnetic resonance (CMR). Despite all, the diagnosis and management of VHD is still mainly based on expert consensus summarized in the current guidelines (5,6), as the overall level of evidence is scarce mainly due to the lack of a true diagnostic “gold standard” and large randomized clinical

trials. Finally, there is evidence for a wide clinical practice gap in patients with proven VHD as a result of the inadequate translation of the existing guidelines into clinical practice (11,12). This leaves, altogether, much room for improvement in the field of VHD.

1.1 Chronic aortic regurgitation

Chronic aortic regurgitation (AR), characterized by the diastolic backward flow of blood from the aorta into the left ventricle (Figure 1), results from malcoaptation of the aortic valve due to abnormalities of the aortic leaflets, their supporting structures (aortic annulus and root), or both (13-15).

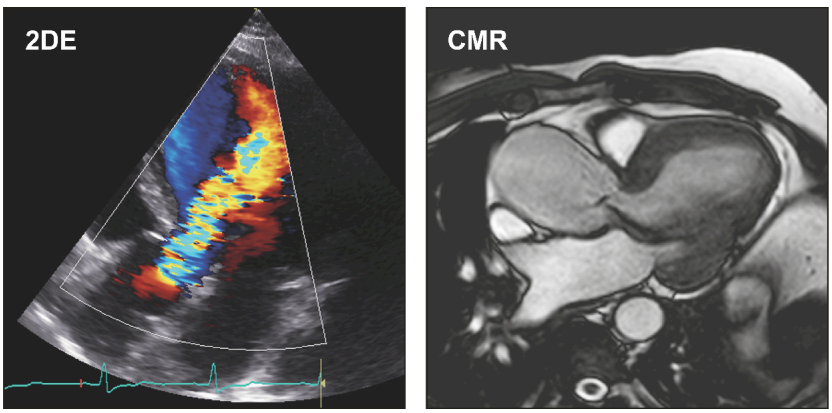

Figure 1 – Visualization of aortic regurgitation using color Doppler echocardiography and cardiovascular magnetic resonance (CMR; balanced steady-state free precession sequence). 2DE, two-dimensional echocardiography

The most common cause of chronic AR in western countries is congenital (bicuspid aortic valve with associated aortic disease) or degenerative disease (such as annuloaortic ectasia) (13,14). The prevalence of AR in western countries ranges from 0.1% in subjects

45-54 years-old to 2% in those ≥ 75 years of age (1). AR is usually discovered by clinical examination, manifested as a characteristic decrescendo diastolic murmur, or incidentally by echocardiography or another non-invasive imaging modality.

Chronic AR is characterized by a combined volume and pressure overload to which the left ventricle responds with a combined eccentric and concentric hypertrophy (16-18). Volume overload is caused by the regurgitant volume (RV), which corresponds with the severity of AR, and pressure overload results from secondary systolic hypertension, which occurs due to an increased total aortic stroke volume, as the normal stroke volume plus RV is ejected into the aorta during systole (16). Furthermore, systolic hypertension is considered to contribute to a cycle of progressive dilatation of the aortic root, which leads to a subsequent worsening of AR (13). The degree of AR is defined by the severity of the valvular lesion (corresponding to the effective regurgitant orifice), the resulting volume overload (quantified as the RV or regurgitant fraction (RF)), the driving force (pressure gradient between the aorta and left ventricle) and the compliance of the left ventricle and ascending aorta. Progression of AR, from mild over moderate to severe regurgitation, is an individual process occurring at a variable pace and involves a complicated interaction of several factors, including AR severity, leaflet and aortic root pathology, as well as the adaptive response of the left ventricle. Mild and moderate AR is both generally benign and even severe AR usually remains asymptomatic for many years. Nonetheless, symptoms are an unreliable marker of AR severity and correlate poorly with left ventricular (LV) dysfunction (19). Morbidity and mortality of the disease is related to the severity of regurgitation, etiology, presence of symptoms, as well as size and function of the

left ventricle (20-25). The overall goal of treatment is the avoidance of death, relief of symptoms, prevention of the development of heart failure and avoidance of aortic complications, which can currently only be achieved by surgical intervention (26). Therefore, surgery is indicated in patients with chronic severe AR who develop symptoms, LV systolic dysfunction, severe LV dilatation and/or severe dilatation of the aortic root or ascending aorta (5,6).

1.2 Chronic mitral regurgitation

Chronic mitral regurgitation (MR), characterized by the systolic backward flow of blood from the left ventricle into the left atrium (Figure 2), results either from disorders of the valve leaflets (primary/organic MR) or the mitral apparatus due to an altered LV geometry (secondary/functional MR) (13-15). In the following, we will focus on primary MR, which is in the western world most frequently caused by degenerative valve disease, with an estimated incidence of

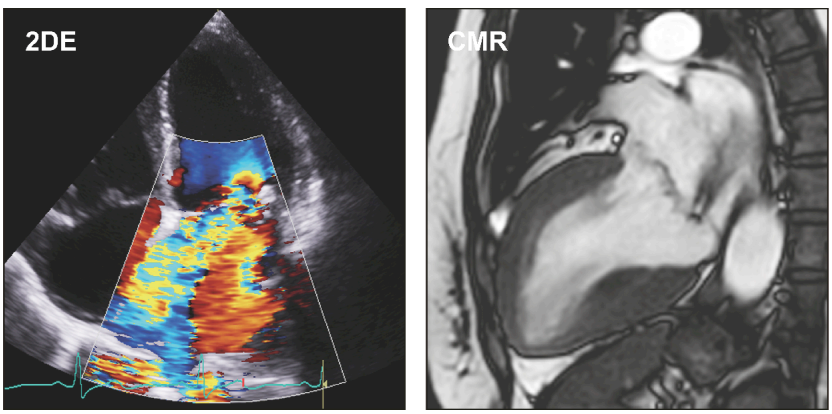

Figure 2 – Visualization of mitral regurgitation using color Doppler echocardiography and cardiovascular magnetic resonance (CMR; balanced steady-state free precession sequence). 2DE, two-dimensional echocardiography

2 to 3 % (2,27). The most common finding in degenerative mitral valve disease is leaflet prolapse, caused by elongation or rupture of the chordae tendineae, resulting in leaflet malcoaptation during ventricular contraction and subsequent MR. Mitral valve prolapse, defined as systolic atrial displacement of the mitral valve by a minimum of 2 mm above the mitral annulus, can be an inheritable condition, linked to markers on chromosome 16p11.2-p12.1, 11p15.4 and 13q31.3-q32.1 (28-30). It comprises a wide clinical spectrum, ranging from single chordal rupture with secondary prolapse of an isolated segment in an otherwise healthy valve (fibroelastic deficiency, older patients), to prolapse of multiple segments involving one or both leaflets in a valve with excess tissue and an enlarged mitral annulus (myxomatous degeneration/Barlow's disease, younger patients) (31-35). MR is usually discovered by clinical examination, manifested as a characteristic holosystolic murmur, or incidentally by echo-cardiography or another non-invasive imaging modality.

Chronic MR causes sole volume overload to which the left ventricle responds with eccentric hypertrophy and the left atrium with dilatation (14). The degree of MR is defined by the severity of the valvular lesion (corresponding to the effective regurgitant orifice), the resulting volume overload (quantified as the RV and RF), the driving force (pressure gradient between the left ventricle and atrium) and the compliance of the left atrium. Progression of MR is an individual process occurring at a variable pace and is usually caused by rupture of the elongated chordae, resulting in unsupported leaflet segments and subsequently more severe MR. This occurs in up to 12% of patients over an average follow-up period of 1.5 years, and is more common in men and older patients (36-38). Mild and moderate MR is both considered benign, in contrast to severe MR. Morbidity and

mortality of the disease is related to the severity of regurgitation, presence of symptoms, size of the left atrium, size and function of the left ventricle, as well as development of atrial fibrillation and pulmonary hypertension (39-44). Similar to AR, surgical intervention is currently the most effective way of treating severe primary MR and mitral valve repair is the preferred method, if applicable (45). Surgery is indicated in patients with severe primary MR who develop symptoms, LV systolic dysfunction, severe LV dilatation, new-onset atrial fibrillation and/or severe pulmonary hypertension (5,6). Recently, the concept of earlier surgical intervention has been proposed, although controversy exists whether asymptomatic patients with severe MR and normal LV function should undergo elective mitral valve repair or not (8,34,46).

1.3 Grading of regurgitation severity

Accurate grading of regurgitation severity is of utmost clinical importance, but one of the most difficult problems in VHD mainly due to the lack of a true “gold standard” and the dependence on changing hemodynamic conditions. Grading of regurgitation severity is important since mild regurgitation does not lead to remodeling of the cardiac chambers, whereas severe regurgitation is associated with substantial remodeling, morbidity and mortality (Figure 3) (20-25,39-44). Historically, angiography has been widely used for the grading of regurgitation severity, even as a reference method for echocardiography and CMR (47-53). However, angiographic grading itself has several limitations and is, nowadays, considered inferior to echocardiography and CMR. Echocardiography is currently the first-line diagnostic tool for the grading of regurgitation severity and CMR

the second-line diagnostic tool in cases of echocardiographic uncertainty (5,6). Regurgitation severity grades, which have historically ranged between three and five grades, are presently, according to a widely accepted consensus, classified into three grades, namely mild, moderate and severe (Figure 3) (5,6,54-56).

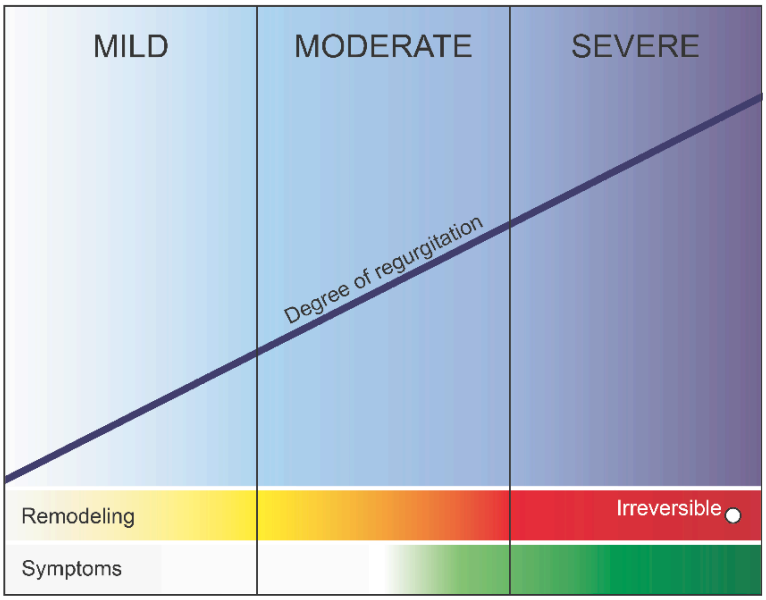

Figure 3 – Grading of regurgitation severity as mild, moderate and severe, including the development of cardiac remodeling and symptoms in relation the regurgitation severity.

Consequently, to assure appropriate clinical decision-making and timing of intervention, non-invasive imaging techniques are needed that can accomplish the grading of regurgitation severity with high precision and reproducibility. Nonetheless, interpretation of the imaging results should always be performed in the clinical context at the time of examination.

1.4 Echocardiography

Echocardiography is currently, as previously mentioned, the first-line diagnostic tool in the evaluation of VHD and uses an “integrative approach” of several qualitative, semi-quantitative and quantitative parameters for the grading of regurgitation severity (5,6,54-56). However, due to feasibility and reproducibility issues, especially when using parameters based on color Doppler echocardiography, grading of regurgitation severity is often challenging and sometimes only based on relatively few parameters (57,58). Furthermore, current guidelines provide no information concerning the weighting of the different parameters and how to approach cases of diagnostic incongruence.

The assessment of LV linear and volumetric dimensions is an integral part in the evaluation of patients with both chronic AR and MR (5,6,54-56). Although LV dilatation is a hallmark of severe chronic regurgitation and LV volumes are an additional valuable quantitative parameter in the “integrative approach”, so far current guidelines include only thresholds for LV linear dimensions indicating severe LV dilatation secondary to severe regurgitation with poor prognosis. In contrast, no thresholds are reported for LV linear and volumetric dimensions indicating severe regurgitation. The most commonly used method for the assessment of LV dimensions is two-dimensional echocardiography (2DE), which nonetheless underestimates LV volumes significantly and has a lower reproducibility compared with CMR (59,60). Real-time three-dimensional echocardiography (RT3DE) overcomes some of the limitations of 2DE and is therefore considered to provide higher levels of agreement and reproducibility compared with CMR (61-63). Nonetheless, RT3DE still

underestimates LV volumes significantly (64). CMR provides currently the most exact assessment of LV volumes with high reproducibility and has been validated extensively as a reference method ("gold standard") (65,66). So far, the thresholds of the established echocardiographic quantitative parameters have been determined in comparison with angiography or other echocardiographic parameters (57,67,68). To establish 2DE and RT3DE thresholds for LV linear and volumetric dimensions indicating severe chronic AR or MR, we decided to use a novel approach by prospectively characterizing patients with moderate AR or MR (as determined by 2DE) as well as patients with severe AR or MR (as determined by 2DE), undergoing surgery according to current guideline criteria, by 2DE and RT3DE, using CMR as the reference method (**Paper I**). Severe LV dilatation was defined as an end-diastolic volume (EDV) index above the 50th percentile obtained by CMR in patients with hemodynamically significant AR or MR and proven surgical benefit. To assure that LV dilation was solely due to valvular regurgitation, patients with confounding causes of LV enlargement were excluded from the study.

As previously mentioned, 2DE and to a lesser degree RT3DE underestimate LV volumes significantly in comparison with CMR. Several plausible causes contributing to this inter-modality discrepancy have been postulated. They include LV foreshortening, off-axis views (69,70), inferior image quality (71), use of geometrical assumptions for the volumetric calculations (70), differences in the endocardial border position and lower spatial resolution by echocardiography (72), as well as insufficient compensation for basal through-plane motion by CMR (73). In contrast, little is known about the ability of the different modalities to delineate simpler LV dimensions like diameter and area. We hypothesized that

underestimation of the LV dimensions by 2DE and RT3DE in comparison with CMR already occurs at the level of the one-dimensional parameters like diameter and increases successively via two-dimensional parameters like area to three-dimensional parameters like volume. Through the systematic study of parameters with increasing complexity (diameter – area – volume), in a multimodality phantom model as well as *in vivo*, we hoped to gain a clearer picture of the main cause of echocardiographic underestimation, assuming that the simplest one-dimensional parameters are influenced by a lesser degree of interfering factors (**Paper II**).

1.5 Cardiovascular magnetic resonance

CMR is currently, as previously mentioned, used as a second-line diagnostic tool and can also provide a comprehensive assessment of chronic AR and MR severity (5,74-76). The assessment of regurgitation severity by CMR is mainly based on the quantification of the respective aortic or mitral RV and RF. These parameters can be obtained by different methods using either solely phase-contrast velocity (PC) imaging or a combination of PC imaging and the slice summation technique, which determines LV volumes (53,77-79). The different CMR quantification methods can, according to our experience, differ substantially in their results, suggesting the necessity of quantification method-specific CMR thresholds.

Quantification of MR can be achieved by a direct and three indirect methods. Direct quantification of MR by CMR, using PC imaging, can be challenging due to frequently eccentric, sometimes direction changing and/or multiple high velocity regurgitant jets, which

cause not only difficulties with adequate image plane alignment, but also introduce errors in PC imaging (80). Nonetheless, direct MR quantification has demonstrated good correlation and agreement with indirect CMR methods (80). The most commonly used indirect ('standard') CMR method, which has been shown to correlate well with quantitative Doppler echocardiography (78) and invasive measurements (53), quantifies MR by subtracting the aortic forward flow (AoFF), obtained by PC imaging, from the LV stroke volume (SV), obtained by the slice summation technique. The second indirect 'volumetric' CMR method, which can only be applied in the absence of multivalvular disease and intra-cardiac shunt, quantifies MR by subtracting the right ventricular SV (RVSV) from the LVSV, both obtained by the slice summation technique. This method has shown poorer inter- and intra-observer variability in comparison with the 'standard' method (81). The third indirect 'flow' CMR method, which has been shown to correlate well with color Doppler echocardiography and has demonstrated excellent inter-observer variability (79), quantifies MR by subtracting the AoFF from the mitral inflow (MiIF), both obtained by PC imaging. Although each indirect quantification method has been validated against other techniques in a limited number of small studies, a systematic comparison of all three indirect CMR methods is currently missing in the scientific literature. Accordingly, we systematically compared all three indirect quantification methods in healthy volunteers without MR, functioning as an internal control group, and patients with MR (**Paper III**).

Currently, quantitative grading of regurgitation severity by 2DE and CMR is usually based on the same guideline thresholds (5,54). Previously, different strategies have been used to identify CMR-specific thresholds. One approach has been to search for the best

concordance between echocardiographic and CMR grading of regurgitation severity, which resulted, nonetheless, in contradictory results (82,83). Another approach has been to look for the link between clinical outcome and CMR regurgitation severity (84). Taken together, current evidence, although scarce, indicates that CMR thresholds differ most likely substantially from the recognized guideline thresholds. We used a novel approach to determine CMR- and quantification method-specific thresholds indicating hemodynamically significant chronic AR or MR benefiting from surgery. To establish these modality- and quantification method-specific thresholds, we decided to prospectively characterize patients with severe AR or MR (as determined by 2DE) undergoing surgery (in keeping with current guidelines) as well as patients with moderate AR or MR (as determined by 2DE) using CMR (**Paper IV**). As CMR grading of regurgitation severity uses no “integrative approach” of several parameters, apart from the determined RV and RF, we even set out to determine additional CMR parameters that can support or exclude the diagnosis of hemodynamically significant AR or MR (**Paper IV**). Thereby taking the first step towards a multi-parametric grading approach by CMR.

2 AIMS

The overall aim of this thesis was to shed new light on some of the remaining diagnostic challenges in chronic AR and MR when using 2DE, RT3DE and/or CMR.

Paper I

To establish 2DE and RT3DE thresholds for LV linear and volumetric dimensions indicating severe chronic AR or MR, using CMR as reference method.

Paper II

To investigate the ability of 2DE, RT3DE and CMR to delineate dimensions with increasing complexity (diameter – area – volume) in a linear and volumetric multimodality phantom model, as well as in the left ventricle of healthy volunteers and valvular heart disease patients according to the same principles, and by this to further characterize the main cause of echocardiographic underestimation of LV dimensions.

Paper III

To compare three indirect CMR methods for MR quantification ('standard', 'volumetric' and 'flow' method) to determine their agreement in healthy volunteers without MR and patients with MR, to study their respective inter- and intra-observer variability, and to determine the effect on grading MR severity in relation to the chosen method in a subgroup of operated patients with severe MR.

Paper IV

To identify CMR- and quantification method-specific thresholds for both the RV index and RF indicating hemodynamically significant chronic AR or MR benefiting from surgery, and to determine alternative CMR parameters that can support or exclude the diagnosis of hemodynamically significant AR or MR.

3 METHODS

This chapter is a summary of all methods used in the four papers on which this thesis is based. For more information, please read the methods section of each paper.

3.1 Study population and design

Paper I

This prospective study comprised 44 AR (moderate (n=20), severe (n=24); as determined by 2DE) and 49 MR patients (moderate (n=17), severe (n=32); as determined by 2DE). Subsequent surgical treatment was performed in 23 AR and 25 MR patients with severe regurgitation due to symptoms and/or severe LV remodeling.

Paper II

The study comprised a phantom and an *in vivo* analysis of 20 healthy volunteers and 25 patients with single moderate or severe AR (n=17) and MR (n=8; as determined by 2DE).

Paper III

This study comprised 16 healthy volunteers and 36 MR patients (moderate (n=5), moderate to severe (n=2), severe (n=29); as determined by 2DE). Subsequent surgical treatment was performed in all patients with severe MR due to symptoms and/or severe LV remodeling.

Paper IV

This prospective study comprised 38 AR (moderate (n=15), severe (n=23)) and 40 MR patients (moderate (n=15), severe (n=25)). Subsequent surgical treatment was performed in all patients with severe AR and MR due to symptoms and/or severe LV remodeling.

Exclusion criteria, for all VHD patients in the four studies, were the presence of ≥ moderate regurgitation in any other valve, intra-cardiac shunt, any other form of relevant cardiac disease, irregular heart rhythm or contraindications for CMR imaging. All participants underwent a 2DE, RT3DE and CMR exam within four hours. Special care was taken to assure high image quality and accurate alignment of the image planes. In all operated patients, a second 2DE and CMR exam was performed 10 ± 1 months post surgery in all but eight AR and eight MR patients, who underwent only a post-surgical 2DE exam due to newly obtained relative contraindications for CMR imaging (permanent pacemaker, mechanical valve) or unwillingness to perform a second CMR scan. Part of every non-invasive imaging exam was also the taking of a medical history and the performance of a physical examination. Post-surgical scans and follow-ups were performed in order to confirm that the initial pre-surgical valvular regurgitation was of hemodynamic significance according to the following criteria: reduction in EDV index of ≥ 15% and/or relief of symptoms.

3.2 Echocardiography

2DE and RT3DE were performed using an iE33 or Vivid E9 imaging system equipped with a 2D sector array transducer or 3D matrix array transducer. Image analysis was performed using EchoPAC or QLAB.

Image acquisition, analysis and grading of regurgitation severity were performed according to current guidelines (54-56,85,86). Echocardiographic exams were approved for final analysis when a clear endocardial border was visible in the parasternal long-axis (PLA) and short-axis (SA) view to delineate LV linear dimensions or ≥ 75% of the endocardial border was seen in the respective projections to obtain LV volumetric dimensions (**Paper I and II**).

Standard projections were obtained by 2DE from the parasternal and apical window (85). LV linear dimensions were obtained in the PLA, SA and apical four-chamber (4CH) view, as the visually largest end-diastolic (EDD) and end-systolic diameter (ESD) at the mitral chordae level (**Paper I and II**). LV ejection fraction (EF) from linear data was calculated according to the Teichholz formula (**Paper I**) (87). LV length was acquired in the 4CH view from the level of the insertion of the mitral valve leaflets to the apex (not included in the published article, **Paper II**). The end-diastolic (EDA) and end-systolic area (ESA) was obtained in the SA and 4CH view (**Paper II**). In **Paper II**, LV linear and areal dimensions were obtained by including both the papillary muscles and trabeculae in the LV cavity to assure identical endocardial border definition criteria across the modalities. In contrast, in **Paper I**, LV linear dimensions were obtained according to 2DE guidelines (85). LV volumetric dimensions were acquired according to the biplane method of disks to determine the EDV and end-systolic volume (ESV) (85). In general, the analysis was performed according to 2DE guidelines, including only the papillary muscles into the LV cavity (85), but also according to RT3DE guidelines (**Paper II**), including both papillary muscles and trabeculae in the LV cavity (Figure 4) (86). The LVEF was calculated as (EDV-ESV)/EDV x 100%.

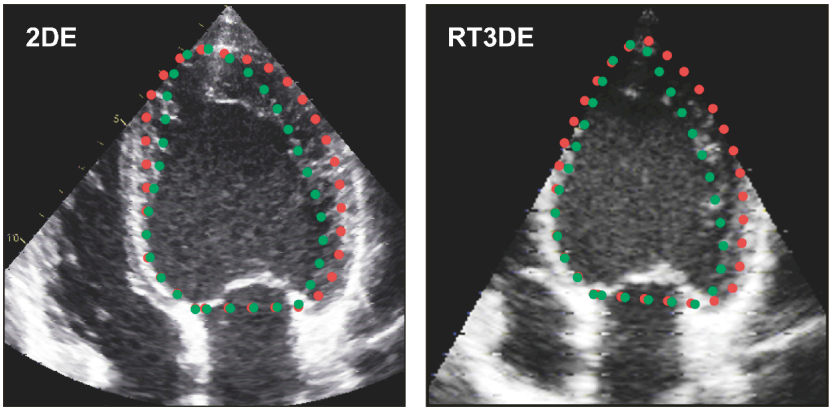

Figure 4 – Delineation of left ventricular volumes using two-dimensional (2DE) and real-time three-dimensional echocardiography (RT3DE), with respect to the exclusion (green dotted lines) or inclusion (red dotted lines) of the trabeculae in the left ventricular cavity.

A full-volume scan was obtained from the apical window by RT3DE during a single breath-hold. Subsectors of the image were acquired over four to six consecutive heartbeats and then subsequently "stitched" together electronically (86). LV linear (including length, not included in the published article) and areal dimensions were measured as for 2DE from the reconstructed SA and long-axis (LA) views derived from the three-dimensional full-volume data set (**Paper II**). Volumetric dimensions were obtained using a semi-automated border detection software with a manual correction function generating a three-dimensional endocardial shell of the LV from which the EDV and ESV were derived on the basis of the voxel count inside the generated mesh (88,89). In general, the analysis was performed according to RT3DE guidelines, including both papillary muscles and trabeculae in the LV cavity (86), but also according to 2DE guidelines (**Paper II**), including only the papillary muscles into the LV cavity (Figure 4) (85). The LVEF was calculated as for 2DE.

3.3 Cardiovascular magnetic resonance

CMR imaging was performed using a 1.5 Tesla scanner with a Q-body coil (phantom model) or five-channel phased-array cardiac coil (*in vivo*). Cine images were acquired using balanced steady-state free precession sequences, with artificial electrocardiography (ECG) gating and without parallel imaging (phantom model), or with retrospective ECG gating and parallel imaging during gentle expiratory breath-hold (*in vivo*). The quantification of the aortic, pulmonary and mitral flow was performed using through-plane PC sequences with retrospective ECG gating during gentle expiratory breath-hold. PC images were acquired perpendicularly aligned to the direction of the blood flow in the aortic root at the level of the sinotubular junction (Figure 5B), the pulmonary trunk just above the pulmonary valve (Figure 5C) and the mitral valve approximately 1 cm below the mitral annulus (ventricular side; Figure 5D) (79,90,91).

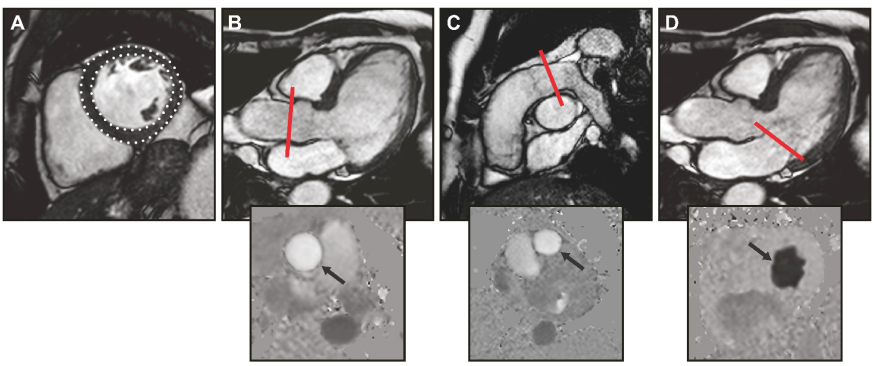

Figure 5 – **(A)** Delineation of the end-diastolic left ventricular endo- and epicardial border (white dots) in the continuous short-axis stack to determine ventricular volumes and mass. **(B and C)** Three-chamber and right-ventricular outflow tract view in end-diastole, illustrating the slice position for through-plane phase-contrast velocity (PC) imaging (red line), including corresponding PC images, to quantify aortic and pulmonary flow (black arrows). **(D)** Three-chamber view in early diastole, illustrating the position for through-plane PC imaging (red line), including corresponding PC image, to quantify mitral inflow (black arrow).

The potential for background phase errors (BPE) was reduced by ensuring that the region of interest (ROI) was for all PC sequences aligned in the isocenter of the magnet to minimize magnetic field inhomogeneities (90). The initially set velocity encoding range (VENC) was subsequently optimized, either in the presence of aliasing or when the difference between the initially set VENC and the determined maximal velocity was > 25% (92). PC images were in all positions performed twice (results are therefore presented as the mean of the two measurements). In all studies, the coefficient of variation of repeated flow measurements was in the aortic, pulmonary and mitral position 5%, 5% and 4% respectively. In all PC measurements, effective compensation for BPEs was applied using adaptive image filtering (93-95). After compensation, the BPE was in all PC images (static tissue) below the current limit of acceptance, namely < 0.6 cm/s (96). Image analysis was performed using ViewForum.

CMR acquired after standardized patient-specific planning a series of cine images in the SA view covering the whole heart without gap from the atrioventricular ring to the apex, followed by cine images in the common long-axis projections (91). LV linear (including length, not included in the published article) and areal dimensions were obtained as for 2DE (**Paper II**). LV volumetric dimensions and mass were obtained by manual tracing of the endocardial and epicardial contour in end-diastole in the successive SA slices of the continuous SA stack (Figure 5A). Endocardial contours were subsequently propagated through all phases using a semi-automated tracing algorithm, followed by manual adjustment, if necessary. Basal through-plane motion was compensated for according to a previously described method by Alfakih et al. (97). Right ventricular volumes

were acquired by manual tracing of the endocardial contour in the end-diastolic and end-systolic frames in the successive SA slices of the continuous SA stack (**Paper III**). In the basal slice, only portions below the pulmonary valve were included in the volume and sections with a thin, non-trabeculated wall were excluded as it was considered part of the right atrium (97). Papillary muscles and trabeculae were included in both the left and right ventricular cavity. The EDV and ESV were automatically computed by the slice summation method. LVSV and EF were calculated as SV = EDV-ESV, and EF = SV/EDV x 100%. The left atrial area (LAA) was determined in end-systole in the 4CH and two-chamber projection (results are presented as the mean of both measurements; **Paper IV**). Aortic and pulmonary flow was determined by delineating the ROI on the respective magnitude image, copied onto the phase image and propagated through all phases using a semi-automated tracing algorithm, followed by manual adjustment, if necessary. Delineation of the mitral valve was performed manually for all phases and in case of a closed valve, flow was zeroed by the delineation of an extremely small ROI on the closed valve (**Paper III and IV**). By integrating the velocity of each pixel in the delineated ROI over one heart cycle, the respective flow information was derived (98).

Quantification of AR was performed first, by direct flow quantification in the aortic root at the level of the sinotubular junction (**Paper I and IV**) (90), and second, by indirect quantification of the RV subtracting the pulmonary stroke volume (PuSV) from the LVSV (**Paper IV**). The quantification of MR was performed first according to the ‘standard’ method, which calculates the RV by subtracting the AoFF from the LVSV (**Paper I, III and IV**) (53,78). Second, by the ‘volumetric’ method, which can only be applied in the absence of

multivalvular disease and intra-cardiac shunt, calculating the RV by subtracting the RVSV from the LVSV (**Paper III**) (80,81). Third, by the 'flow' method, which calculates the RV by subtracting the AoFF from the MiIF (**Paper III and IV**) (79). In general, RFs were calculated as follows: RV/LVSV x 100% or RV/MiIF x 100%. In **Paper III**, eight MR patients had ≥ mild pulmonary and/or tricuspid regurgitation (as determined by 2DE) and were therefore excluded from MR quantification using the 'volumetric' method. Otherwise, all other quantification methods could be applied in all participants. Grading of AR and MR severity was performed according to current guideline thresholds (5).

3.4 Multimodality phantom model

The multimodality phantom model, built out of polycarbonate, consists of an open cube (160 x 160 x 160 mm) that can be modified to a linear model by inserting two centered plates with adjustable predefined distances (initial centered spacing 10 mm, followed by a continuous increase in distance of 10 mm, max. analyzed distance 100 mm) or to a volumetric model by inserting a centered cylinder with a predefined central volume (diameter 44 mm, length 66 mm, SA area 16 cm^2, LA area 29 cm^2, volume 100 ml; Figures 6A-C; **Paper II**). Sufficient contrast was achieved by adding potato flour to the water-filled phantom model for 2DE/RT3DE and manganese (II) chloride doped water for CMR.

For 2DE and RT3DE both phantom models were analyzed with the transducer centered on the bottom plate, corresponding to an apical LA projection (position II), and with the transducer centered on a thin side plate, corresponding to a parasternal SA projection

(position I, Figures 6B-E). The linear phantom model was examined by determining the distance between the plates in LA (at five different points of measurement) and SA projections (Figures 6B and 6D). The volumetric phantom model was analyzed in LA and SA projections concerning diameter (not included in the published article), length (not included in the published article) and area (Figure 6C and 6E). Volumetric dimensions were acquired for both 2DE and RT3DE according to a geometrical cylinder model (π x radius^2 x length; not included in the published article) and the biplane method of disks, and for RT3DE also according to a mesh-based volumetric method.

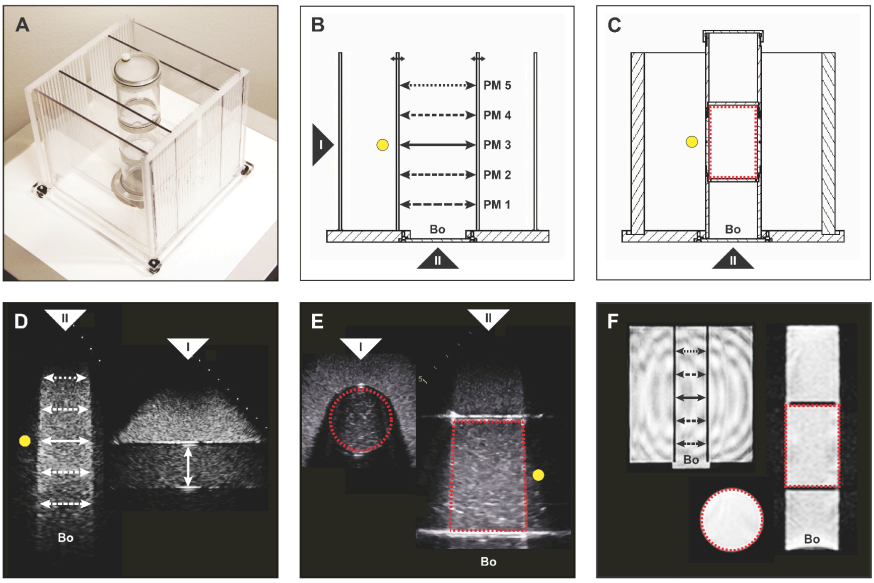

Figure 6 – Image and schematic drawing of the linear and volumetric multimodality phantom model **(A-C)**. Echocardiographic assessment was performed with the transducer centered on the side plate (I) and with a transducer centered on the bottom plate (II). Examples of the analysis of the linear **(D/F)** and volumetric model **(E/F)** by two-dimensional echocardiography and cardiovascular magnetic resonance respectively. Black and white arrows – linear dimensions; Red dotted lines – areal dimensions; Bo – bottom plate; PM – point of measurement; Yellow point – focus position. Reproduced with permission of the publisher.

CMR acquired continuous images without gap in the sagittal and transverse planes of the linear and volumetric phantom model. The linear and volumetric phantom model was examined according to the same principles as 2DE/RT3DE in terms of diameter and area (Figures 6B, 6C and 6F). Volumetric dimensions were determined using a geometrical cylinder model (not included in the published article) and the slice summation method.

3.5 Reproducibility analysis

Inter-observer variability was assessed in an independent analysis by a second observer and intra-observer variability was determined in an independent second analysis by the primary observer. Both observers were blinded to previous results.

3.6 Statistical analysis

Agreement between methods was evaluated using the Bland-Altman method by calculating the mean difference (MD) ± standard deviation (SD) and limits of agreement (LoA; MD ± 1.96 SD) (99). Correlation was assessed using the Pearson's or Spearman's rank correlation coefficient. The significance of the differences between the modalities was assessed using a Friedman's test to determine the overall P-value (values of < 0.05 were considered significant), followed by a post-hoc analysis using a Wilcoxon signed rank test when the initial null hypothesis was rejected (P-values of < 0.016 were considered significant (Bonferroni correction)). Otherwise, a paired Student's t-test or Wilcoxon signed rank test was used for the comparison of dependant groups and a Mann-Whitney U test for the comparison of

independent groups. Receiver operating characteristics curve (ROC) analysis was performed to establish diagnostic thresholds (100). The diagnostic performance of the individual thresholds was assessed using sensitivity, specificity, positive likelihood ratio (PLR) and negative likelihood ratio (NLR) (101,102). The PLR is the ratio between the probability of a positive test result in patients with disease and the probability of a positive test result in those without disease (sensitivity/(1-specificity)). The NLR is the ratio between the probability of a negative test result in patients with disease and the probability of a negative test result in those without disease ((1-sensitivity)/specificity). Inter- and intra-observer variability was assessed by the coefficient of variation (defined as the (SD of the differences between observer measurements/mean of the observer measurements) x 100) and repeatability coefficient (defined as 1.96 x √(sum of the squares of the differences between observer measurements/n)) (99,103). The significance of the squared differences in the repeatability coefficient was assessed as above by a Friedman's test followed, if applicable, by a Wilcoxon signed rank test or by solely a Wilcoxon signed rank test. Statistical analysis was performed using IBM SPSS Statistics 19.

3.7 Ethical considerations

All studies were conducted according to the Declaration of Helsinki. The Regional Ethics Review Board in Gothenburg gave ethical approval for the study protocols, and written informed consent was obtained from all participants.

4 RESULTS

This chapter is a summary of the main results presented in the four papers on which this thesis is based. For more information, please read the results section of each paper.

4.1 Paper I

Each included patient had no other underlying cause contributing to LV dilation apart form single VHD. All operated patients experienced a reduction in EDV index ≥ 15% and/or relief of symptoms. EDD_{2DE}, EDV_{2DE} and EDV_{CMR} could be obtained in all participants (n = 93). In contrast, EDV_{RT3DE} was only obtained in 71 patients (76%) that fulfilled the analysis criteria.

Linear and volumetric dimensions in AR and MR patients

The EDD_{2DE}, obtained in the PLA, was similar in patients with AR and MR (59 ± 6.1 mm versus 58 ± 6.0 mm, P = 0.49). In contrast, the EDV between AR and MR patients were significantly different for 2DE (197 ± 73 ml versus 148 ± 41 ml, P < 0.0001), RT3DE (220 ± 61 ml versus 184 ± 41 ml, P = 0.005) and CMR (310 ± 95 ml versus 263 ± 60 ml, P = 0.001).

Comparison of LV dimensions obtained by 2DE, RT3DE and CMR

The overall linear relationship between EDD_{2DE} and EDV_{CMR} was moderate (n = 93, r = 0.73, P < 0.0001). Furthermore, the overall linear relationship between EDV_{2DE} and EDV_{CMR} as well as EDV_{RT3DE}

and EDV_{CMR} was strong (Figure 7). 2DE underestimated EDVs significantly in comparison with CMR and the limits of agreement were wide. This was to a lesser extent also the case when comparing RT3DE with CMR (Figure 7 and 8). There was no difference in the obtained LVEF between 2DE and CMR. In contrast, RT3DE determined a significantly lower LVEF compared with 2DE and CMR.

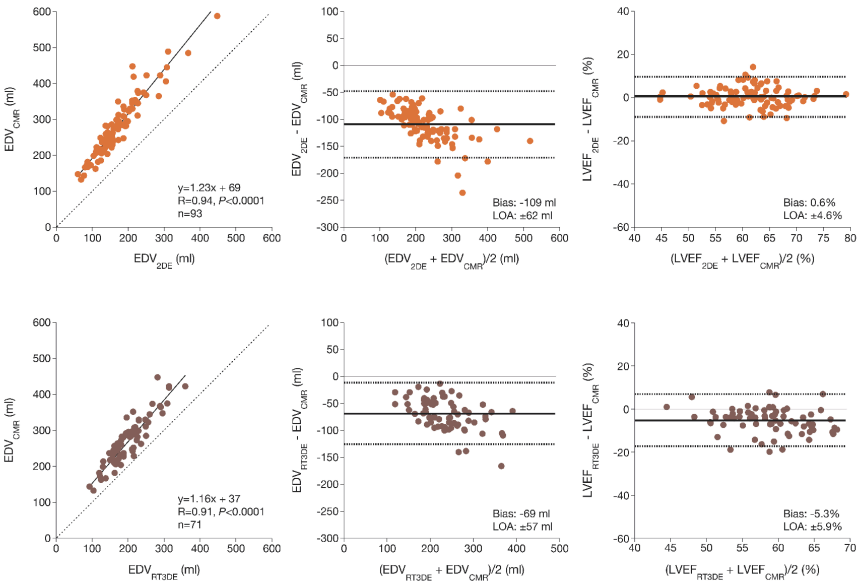

Figure 7 – Scatterplots and Bland-Altman analyses illustrating the relation between end-diastolic volume (EDV) and left ventricular ejection fraction (LVEF) obtained by two-dimensional echocardiography (2DE) versus cardiovascular magnetic resonance (CMR; upper three plots) and real-time three-dimensional echocardiography (RT3DE) versus CMR (lower three plots). Dashed lines indicate the line of identity or the 95% limits of agreement (LOA). Horizontal solid lines represent the mean difference (bias). R, correlation coefficient

Identification of severe LV dilatation

Severe LV dilation was defined as an EDV_{CMR} index above the 50th percentile in patients undergoing surgery for severe AR or MR.

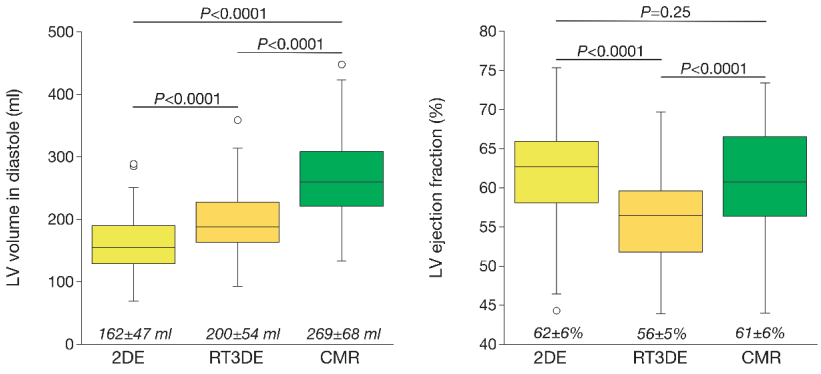

Figure 8 – Comparison of the determined left ventricular (LV) end-diastolic volumes and ejection fractions (n=71) obtained by two-dimensional (2DE), real-time three-dimensional echocardiography (RT3DE) and cardiovascular magnetic resonance (CMR). The overall P-value, when comparing all three modalities, was < 0.0001 for both parameters. The significance of the differences between the modalities is presented as P values.

Table 1 – Diagnostic performance of thresholds indicating marked LV dilatation defined as EDV_{CMR} index above the 50th percentile

	AUC (95% CI)	**Threshold**	**Sensitivity** (95% CI)	**Specificity** (95% CI)	**PLR** (95% CI)	**NLR** (95% CI)
Aortic regurgitation						
EDD index (cm/m^2)	0.86 (0.74 – 0.97)	> 3.0	73 (48 – 89)	83 (65 – 92)	4.3 (1.8 – 9.9)	0.32 (0.14 – 0.8)
EDV_{2DE} index (ml/m^2)	0.97 (0.92 – 1.0)	> 100	93 (70 – 99)	97 (83 – 99)	27 (3.9 – 187)	0.07 (0.01 – 0.46)
EDV_{RT3DE} index (ml/m^2)	0.99 (0.96 – 1.0)	> 115	88 (53 – 98)	92 (74 – 98)	10.5 (2.7 – 41)	0.14 (0.02 – 0.86)
Mitral regurgitation						
EDD index (cm/m^2)	0.71 (0.56 – 0.85)	> 3.0	63 (39 – 82)	64 (47 – 78)	1.7 (0.9 – 3.1)	0.59 (0.30 – 1.2)
EDV_{2DE} index (ml/m^2)	0.94 (0.88 – 1.0)	> 80	88 (64 – 97)	91 (76 – 97)	9.6 (3.2 – 29)	0.14 (0.04 – 0.5)
EDV_{RT3DE} index (ml/m^2)	0.89 (0.78 – 0.99)	> 99	83 (55 – 95)	77 (58 – 89)	3.6 (1.7 – 7.6)	0.22 (0.06 – 0.8)

AUC, area under the curve; CI, confidence interval; CMR, cardiovascular magnetic resonance; EDD, end-diastolic diameter; EDV, end-diastolic volume; NLR, negative likelihood ratio; PLR, positive likelihood ratio; RT3DE, real-time three-dimensional echocardiography; 2DE, two-dimensional echocardiography

In patients with AR the 50th percentile for the EDV_{CMR} index was 161 ml/m^2 and the corresponding for MR was 135 ml/m^2. The ability of 2DE and RT3DE to identify severe LV dilatation was tested using ROC analyses for AR and MR separately. The area under the curve was large for both 2DE and RT3DE EDV indices and moderate to large for the EDD indices (Table 1). In both AR and MR, LV linear dimensions could not sufficiently identify patients with severe LV dilatation. In AR, the diagnostic ability was excellent for both 2DE and RT3DE LV volumes with a PLR ≥ 10. In MR, the diagnostic ability was overall weaker than in AR and only the 2DE LV volumes displayed a good diagnostic ability with a PLR ≥ 5 (Table 1).

4.2 Paper II

Linear and volumetric phantom model

2DE and RT3DE depicted the linear dimensions of the linear and volumetric phantom model in the SA projection with similar precision as CMR, and in the LA projection in a depth-dependant manner with the smallest absolute error (actual dimension – measured dimension) at the level of the focus position (Figure 9). Otherwise, all three modalities depicted the areal and volumetric dimensions of the volumetric phantom model with high precision (Figure 9).

Left ventricular dimensions *in vivo*

The image acquisition protocol was successfully completed in all participants. Nonetheless, the obtained data sets did not fulfill the strict echocardiographic analysis criteria in all cases and for all parameters (Table 2). Patients without sufficiently acquired 2DE and

RT3DE data sets (apical window) had significantly larger EDVs obtained by CMR than data sets of patients fulfilling the analysis criteria (373 ± 118 ml versus 274 ± 51 ml (P = 0.02) and 404 ± 110 ml versus 269 ± 46 ml (P = 0.001) respectively).

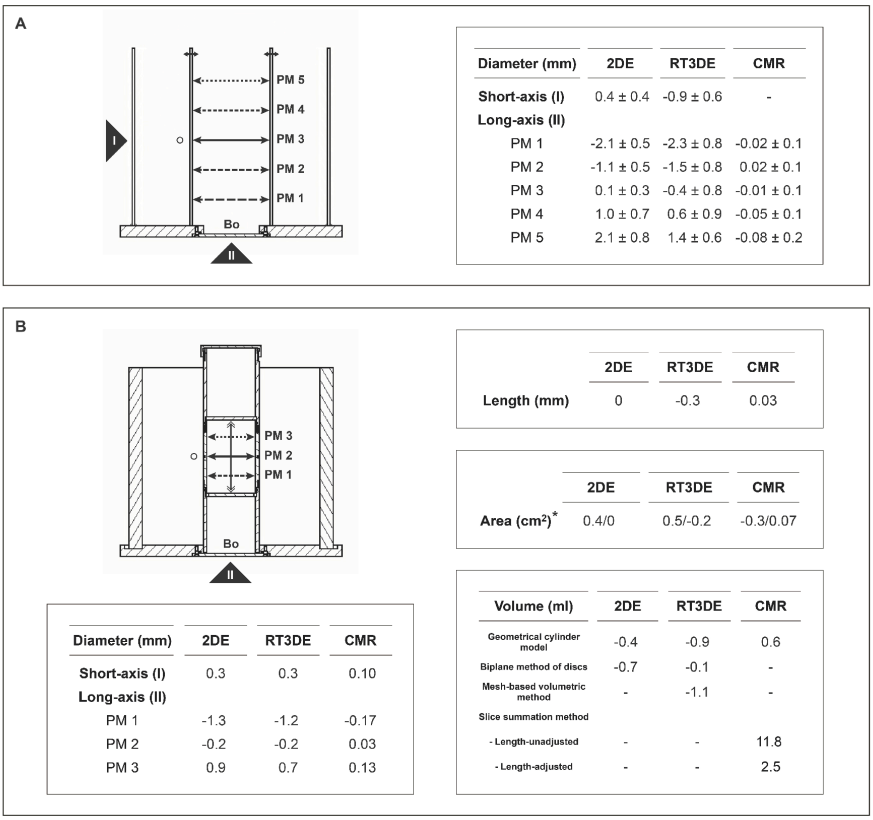

Diameter (mm)	2DE	RT3DE	CMR
Short-axis (I)	0.4 ± 0.4	-0.9 ± 0.6	-
Long-axis (II)			
PM 1	-2.1 ± 0.5	-2.3 ± 0.8	-0.02 ± 0.1
PM 2	-1.1 ± 0.5	-1.5 ± 0.8	0.02 ± 0.1
PM 3	0.1 ± 0.3	-0.4 ± 0.8	-0.01 ± 0.1
PM 4	1.0 ± 0.7	0.6 ± 0.9	-0.05 ± 0.1
PM 5	2.1 ± 0.8	1.4 ± 0.6	-0.08 ± 0.2

	2DE	RT3DE	CMR
Length (mm)	0	-0.3	0.03

	2DE	RT3DE	CMR
Area (cm^2)*	0.4/0	0.5/-0.2	-0.3/0.07

Diameter (mm)	2DE	RT3DE	CMR
Short-axis (I)	0.3	0.3	0.10
Long-axis (II)			
PM 1	-1.3	-1.2	-0.17
PM 2	-0.2	-0.2	0.03
PM 3	0.9	0.7	0.13

Volume (ml)	2DE	RT3DE	CMR
Geometrical cylinder model	-0.4	-0.9	0.6
Biplane method of discs	-0.7	-0.1	-
Mesh-based volumetric method	-	-1.1	-
Slice summation method			
- Length-unadjusted	-	-	11.8
- Length-adjusted	-	-	2.5

Figure 9 – Dimensions of the linear (A) and volumetric multimodality phantom model (B) assessed by two-dimensional echocardiography (2DE), real-time three-dimensional echocardiography (RT3DE) and cardiovascular magnetic resonance (CMR). The linear phantom model dimensions (A) are presented as the mean absolute error (AE) ± standard deviation (SD; mean of all acquired distances from 10 to 100 mm) at each point of measurement (PM). The assessed dimensions of the volumetric phantom model (B) are presented as the AE ± SD concerning diameter (at each PM), length, area (* short-axis/long-axis) and volume (using different methods). Black arrows – linear dimensions; Circle – focus position. Otherwise, abbreviations and symbols as in Figure 6

2DE underestimated the SA-EDD (Table 2) and 4CH-EDD (MD ±

SD: -2 ± 4 mm, p = 0.01) significantly compared with CMR, but not the SA-ESD (Table 2). RT3DE underestimated the linear dimensions to an even higher degree than 2DE (Table 2). In comparison with CMR, 2DE (MD ± SD: -7 ± 5 mm) and RT3DE (MD ± SD: -8 ± 5 mm) underestimated the 4CH-LV length significantly (Table 3).

Table 2 – Comparison of LV dimensions between 2DE, RT3DE and CMR

					Post-hoc analysis		
	2DE *	**RT3DE ***	**CMR ***	**Overall P-value**	**2DE vs RT3DE**	**2DE vs CMR**	**RT3DE vs CMR**
Diameter (mm)							
SA-EDD	63 ± 9 (35)	59 ± 7 (23)	65 ± 10 (45)	< 0.0001 (19)	< 0.0001	< 0.0001	< 0.0001
SA-ESD	44 ± 7 (34)	40 ± 5 (20)	45 ± 9 (45)	0.001 (16)	< 0.0001	0.52	0.03
Area (cm^2)							
SA-EDA	28 ± 9 (24)	25 ± 5 (21)	33 ± 10 (45)	< 0.0001 (12)	0.002	< 0.0001	< 0.0001
SA-ESA	15 ± 5 (27)	13 ± 3 (19)	16 ± 7 (45)	0.01 (11)	0.003	0.12	0.04
Volume (ml)							
EDV	171 ± 58 (24)	171 ± 50 (25)	250 ± 107 (45)	< 0.0001 (21)	0.57	< 0.0001	< 0.0001
ESV	72 ± 27 (24)	72 ± 22 (25)	99 ± 52 (45)	< 0.0001 (21)	0.96	< 0.0001	< 0.0001

* Data are presented as the mean ± standard deviation (number of analyzed patients with adequate image quality). The significance of the differences between two-dimensional echocardiography (2DE), real-time three-dimensional echocardiography (RT3DE) and cardiovascular magnetic resonance (CMR) are presented as P-values (number of patients contributing to the paired comparisons). For all analyzed parameters and modalities, both papillary muscles and trabeculae were included in the left ventricular (LV) cavity. EDA, end-diastolic area; EDD, end-diastolic diameter; EDV, end-diastolic volume; ESA, end-systolic area; ESD, end-systolic diameter; ESV, end-systolic volume; SA, short-axis; vs, versus. Reproduced with permission of the publisher.

Table 3 – Comparison of the LV length between 2DE, RT3DE and CMR

					Post-hoc analysis		
	2DE *	**RT3DE ***	**CMR ***	**Overall P-value**	**2DE vs RT3DE**	**2DE vs CMR**	**RT3DE vs CMR**
Length (mm)							
4CH	96 ± 10	93 ± 7	104 ± 11	< 0.0001	0.16	< 0.0001	< 0.0001

* Data are presented as the mean ± standard deviation. The significance of the differences between two-dimensional echocardiography (2DE), real-time three-dimensional echocardiography (RT3DE) and cardiovascular magnetic resonance (CMR) are presented as P-values. Both papillary muscles and trabeculae were included in the left ventricular (LV) cavity. 4CH, four-chamber; vs, versus

The 95% limits of agreement between 2DE and CMR were wide for the SA-EDD (MD ± SD: -1 ± 1 mm; LoA: -4 to 2 mm) and even wider for the 4CH-EDD (MD ± SD: -2 ± 4 mm; LoA: -10 to 5 mm).

Compared with CMR, 2DE underestimated the SA-EDA (Table 2) and 4CH-EDA (MD ± SD: -7 ± 4 cm^2, $p < 0.0001$) significantly, but not the SA-ESA (Table 2). Like the linear dimensions, RT3DE underestimated the area to a higher degree than 2DE (Table 2).

2DE and RT3DE underestimated all LV volumes significantly compared with CMR (Table 2). Nonetheless, the degree of underestimation varied depending on the exclusion or inclusion of the trabeculae in the LV cavity (Figure 10).

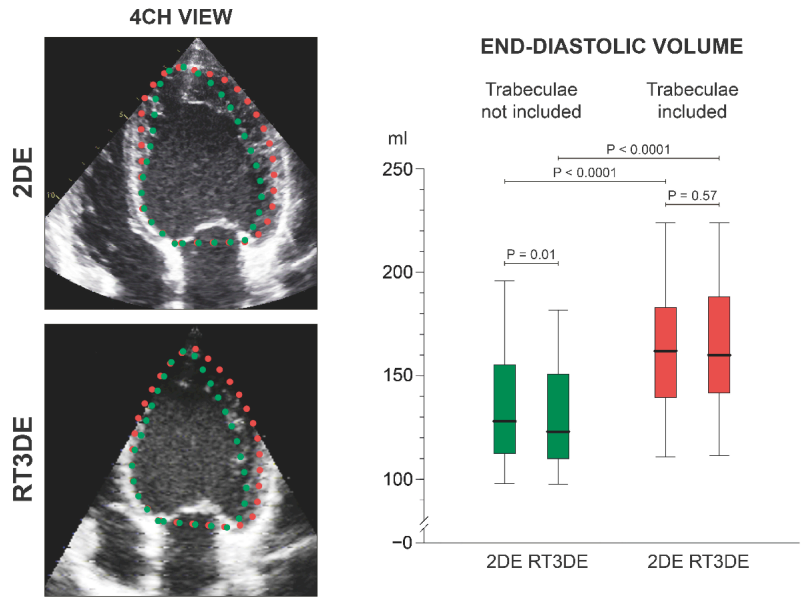

Figure 10 – Differences in the end-diastolic volume (EDV), obtained by two-dimensional (2DE) and real-time three-dimensional echocardiography (RT3DE), depending on the exclusion (green dotted lines and boxes) or inclusion of the trabeculae in the LV cavity (red dotted lines and boxes). The significance of the difference in EDVs is presented as P-value. 4CH, four-chamber. Reproduced with permission of the publisher.

The degree of underestimation increased successively from diameter (on average by 2% for 2DE and 6% for RT3DE) to area (on average by 6% for 2DE and 11% for RT3DE) and finally volume (on average by 18% for both 2DE and RT3DE) when analyzed according to the same principles.

4.3 Paper III

Healthy volunteers without mitral regurgitation

The comparison of the LVSV versus the AoFF ('standard' method, $P < 0.0001$) showed a clear tendency towards LVSV overestimation (Figure 11). In contrast, the comparison of the LVSV versus the RVSV ('volumetric' method, $P = 0.05$) and of the MiIF versus the AoFF ('flow' method, $P = 0.28$) displayed only small differences, as would be expected in healthy volunteers without MR. Nonetheless, all three methods had similarly wide 95% limits of agreement (Figure 11).

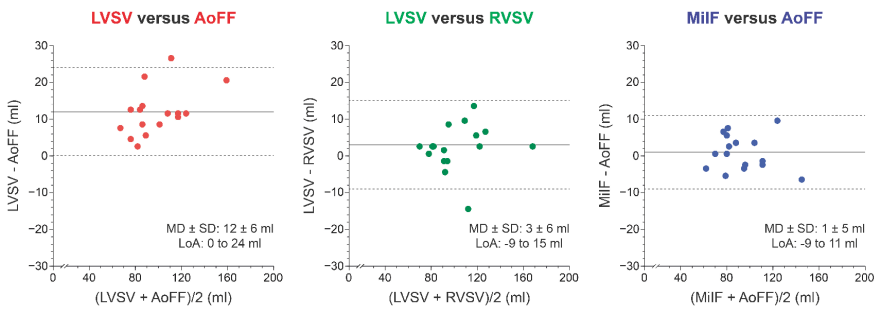

Figure 11 – Bland-Altman comparison of the LVSV versus AoFF ('standard' method, red), LVSV versus RVSV ('volumetric' method, green) and MiIF versus AoFF ('flow' method, blue) in healthy volunteers without MR. AoFF, aortic forward flow; LoA, 95% limits of agreement (dashed lines); LVSV, left ventricular stroke volume; MD, mean difference (solid line); MiIF, mitral inflow; RVSV, right ventricular stroke volume; SD, standard deviation. Reproduced with permission of the publisher.

Patients with mitral regurgitation

The ‘standard’ method determined clearly larger RVs and RFs, in contrast to the ‘volumetric’ and ‘flow’ method, which displayed similar MR quantification results (Table 4 and Figure 12). The 95% limits of agreement were narrowest when comparing the ‘standard’ versus the ‘volumetric’ method, and broadened successively when comparing the ‘standard’ versus the ‘flow’ method and finally the ‘volumetric’ versus the ‘flow’ method (Figure 12).

Table 4 – Comparison of the different indirect MR quantification methods in patients with MR

					Post-hoc analysis		
	LVSV-AoFF	**LVSV-RVSV**	**MiIF-AoFF**	**Overall P-value**	**LVSV-AoFF v LVSV-RVSV**	**LVSV-AoFF v MiIF-AoFF**	**LVSV-RVSV v MiIF-AoFF**
RV (ml)	90 ± 31	76 ± 30	70 ± 32	< 0.0001	< 0.0001	< 0.0001	0.07
RF (%)	51 ± 11	42 ± 11	44 ± 15	< 0.0001	< 0.0001	< 0.0001	0.63

Data are presented as the mean ± standard deviation. The significance of the differences between the different methods is presented as P-values. AoFF, aortic forward flow; LVSV, left ventricular stroke volume; MiIF, mitral inflow; MR, mitral regurgitation; RF, regurgitant fraction; RV, regurgitant volume; RVSV, right ventricular stroke volume; v, versus. Reproduced with permission of the publisher.

The ‘standard’ method obtained in all operated patients with severe MR, as determined by 2DE, a RV above the guideline threshold of ≥ 60 ml. This was also the case for most of the patients when using the ‘volumetric’ and ‘flow’ method (86% (n=19/22) and 83% (n=24/29) above the threshold respectively). In contrast, only the ‘standard’ method determined for most of the patients a RF above the guideline threshold of ≥ 50% (76% (n=22/29)), whereas for the ‘volumetric’ and for the ‘flow’ method, only 32% (n= 7/22) and 48% (n=14/29) of the patients lay above the threshold respectively.

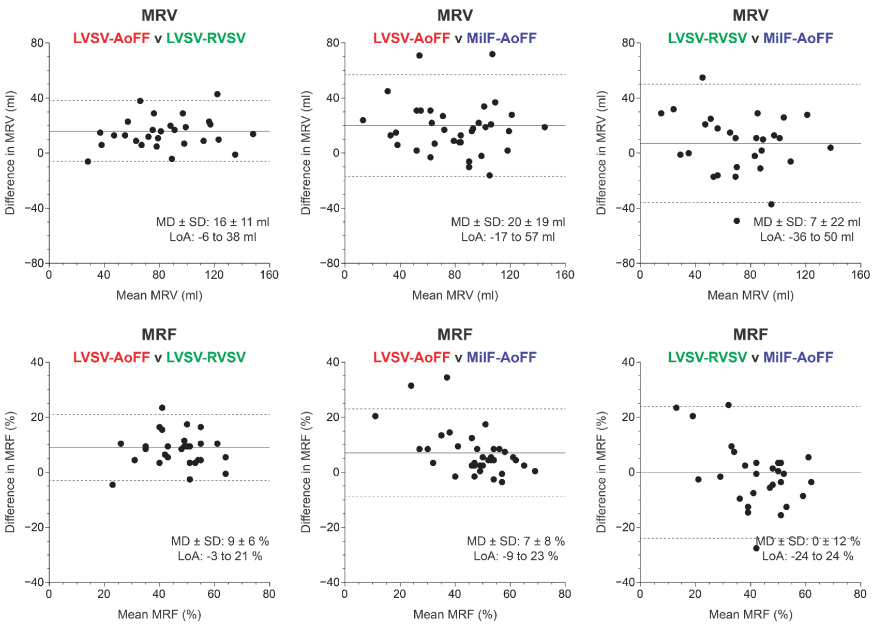

Figure 12 – Bland-Altman comparison of the 'standard' (LVSV-AoFF), 'volumetric' (LVSV-RVSV) and 'flow' (MiIF-AoFF) method in patients with MR concerning the determined mitral regurgitant volume (MRV) and fraction (MRF). AoFF, aortic forward flow; LoA, 95% limits of agreement (dashed lines); LVSV, left ventricular stroke volume; MD, mean difference (solid line); MiIF, mitral inflow; RVSV, right ventricular stroke volume; SD, standard deviation. Reproduced with permission of the publisher.

Inter- and intra-observer variability

Inter-observer variability was lowest for the 'flow' method and increased successively via the 'standard' to the 'volumetric' method (Table 5). In contrast, intra-observer variability was similar for all three methods (Table 5).

Table 5 – Inter- and intra-observer variability of the RV and RF in patients with MR for the different indirect MR quantification methods

	Inter-observer variability		Intra-observer variability	
	CV	RC	CV	RC
LVSV-AoFF				
RV	14	24	5	8
RF	7	7	2	2
LVSV-RVSV				
RV	18	28	7	10
RF	15	12	6	5
MilF-AoFF				
RV	10	14	5	7
RF	7	6	4	4

Data are presented as the coefficient of variation (CV) in percent and the repeatability coefficient (RC) in absolute values (RV in ml, RF in %). AoFF, aortic forward flow; LVSV, left ventricular stroke volume; MilF, mitral inflow; MR, mitral regurgitation; RF, regurgitant fraction; RV, regurgitant volume; RVSV, right ventricular stroke volume. Reproduced with permission of the publisher.

4.4 Paper IV

Patient and CMR characteristics

Patients with severe AR and MR had, compared with moderate regurgitation, significantly larger EDVs (176 ± 48 ml/m^2 versus 127 ± 20 ml/m^2 ($P < 0.0001$) and 140 ± 20 ml/m^2 versus 102 ± 15 ml/m^2 ($P < 0.0001$)), an increased LV mass (98 ± 31 g/m^2 versus 71 ± 15 g/m^2 ($P = 0.001$) and 76 ± 15 g/m^2 versus 57 ± 9 g/m^2 ($P < 0.0001$)) and an increased LAA (MR only: 19 ± 4 cm^2/m^2 versus 14 ± 3 cm^2/m^2 ($P < 0.0001$)). In contrast, no differences were observed regarding the EF. All operated patients with severe AR experienced a reduction in EDV index ≥ 15% and/or relief of symptoms. In case of severe MR, a reduction in the EDV index ≥ 15% was present in all but one patient,

who developed a reduction in the EDV index of 14% but became free of symptoms post-surgery.

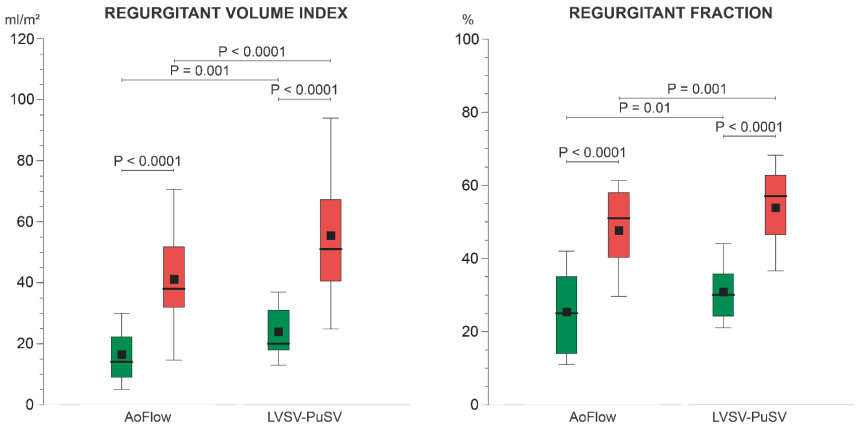

Figure 13 – CMR quantification of moderate (green) and severe (red) aortic regurgitation (AR) using a direct and an indirect method. The significance of the differences between moderate and severe AR as well as direct (AoFlow) and indirect quantification (LVSV-PuSV) is presented as P-values. Black squares represent the mean. AoFlow, aortic flow; LVSV, left ventricular stroke volume; PuSV, pulmonary stroke volume

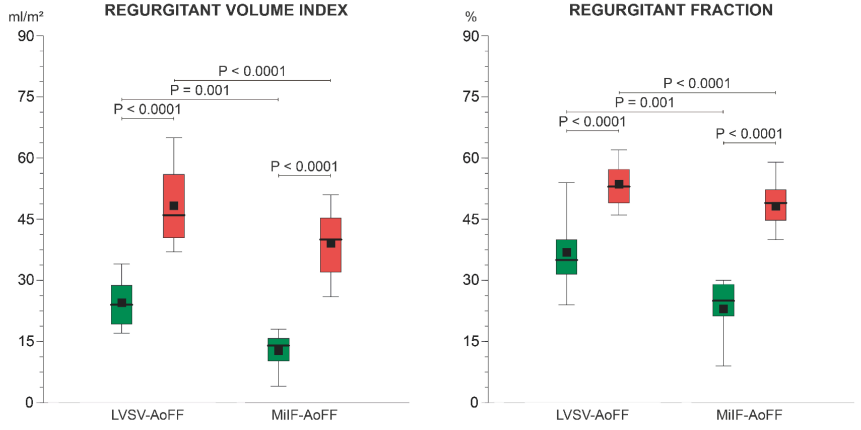

Figure 14 – CMR quantification of moderate (green) and severe (red) mitral regurgitation (MR) using two different indirect methods. The significance of the differences between moderate and severe MR as well as two different indirect quantification methods (LVSV-AoFF versus MiIF-AoFF) is presented as P-values. Black squares represent the mean. AoFF, aortic forward flow; LVSV, left ventricular stroke volume; MiIF, mitral inflow

Independent of the quantification method used, AR and MR patients with severe regurgitation had significantly larger RV indices and RFs than patients with moderate regurgitation (Figure 13 and 14). In both moderate and severe AR, the indirect quantification method (LVSV-PuSV) determined larger RV indices and RFs than the direct quantification method (Figure 13). Furthermore, in both moderate and severe MR, the indirect quantification method using a combination of PC imaging and slice summation technique (LVSV-AoFF) obtained larger RV indices and RFs than the indirect method using solely PC imaging (MiIF-AoFF; Figure 14).

Identification of hemodynamically significant regurgitation benefiting from surgery

In operated patients with severe AR or MR, as determined by 2DE, the application of current guideline RF thresholds led frequently to discordant grading by CMR and was, furthermore, dependant on the CMR quantification method used (Figure 15).

CMR specific thresholds for the EDV index, myocardial mass index (AR only), LAA index (MR only), RV index and RF (for each quantification method) indicating hemodynamically significant AR or MR benefiting from surgery were determined using ROC analyses (Table 6 and 7). The diagnostic accuracy, indicated by the area under the curve, was good in AR and good to excellent in MR.

In AR, the discriminatory ability was strong for the EDV index, the RV index using both methods and the RF using the indirect method with a low NLR (< 0.2). Solely the RV index using the indirect method had also a PLR with a strong discriminatory ability (> 5). The weakest discriminatory power was observed for the myocardial mass index (Table 6).

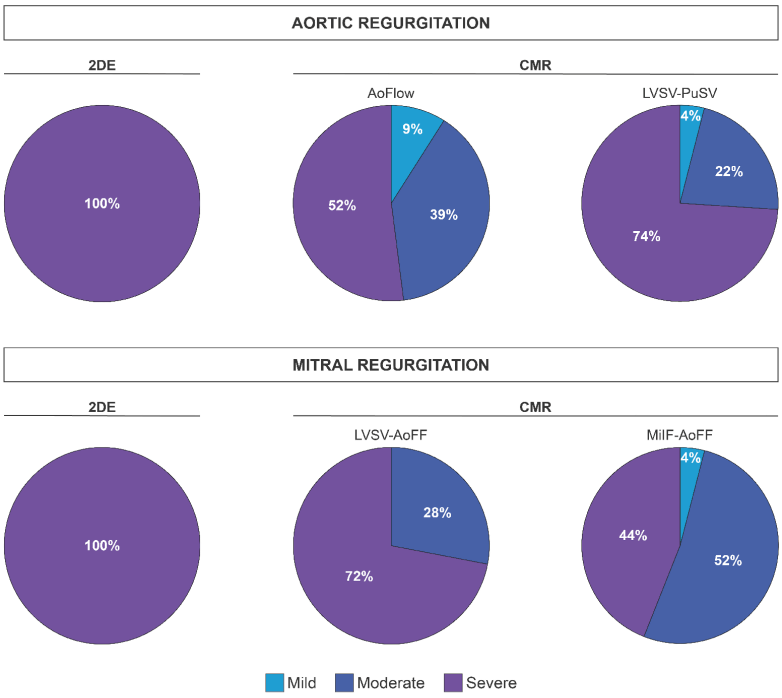

Figure 15 – Discordance between two-dimensional echocardiography (2DE) and cardiovascular magnetic resonance (CMR) in the grading of chronic aortic (AR) and mitral regurgitation (MR). In operated patients with severe AR or MR, as determined by 2DE, the application of current guideline regurgitant fraction thresholds led frequently to discordant grading by CMR in a method-dependant manner.

In MR, the discriminatory power was in general stronger than in AR. The discriminatory ability was very strong for the EDV index, RV index and RF using both methods with a low NLR (< 0.1). Both the EDV index and RF (MiIF-AoFF) showed PLRs with very strong discriminatory abilities (> 10). The strongest discriminatory power was observed for the RV index (MiIF-AoFF) and the weakest for the LAA index (Table 7).

Table 6 – Diagnostic performance of thresholds indicating hemodynamically significant chronic aortic regurgitation benefiting from surgery

	AUC (95% CI)	**Threshold**	**Sensitivity** (95% CI)	**Specificity** (95% CI)	**PLR** (95% CI)	**NLR** (95% CI)
EDV index (ml/m^2)	0.85 (0.72 – 0.98)	> 135	87 (68 – 96)	73 (48 – 89)	3.3 (1.4 – 7.7)	0.18 (0.06 – 0.53)
Mass index (g/m^2)	0.82 (0.68 – 0.96)	> 79	78 (58 – 90)	80 (55 – 93)	3.9 (1.4 – 11.0)	0.27 (0.12 – 0.61)
AoFlow						
RV index (ml/m^2)	0.89 (0.79 – 0.99)	> 20	87 (68 – 96)	73 (48 – 89)	3.3 (1.4 – 7.7)	0.18 (0.06 – 0.53)
RF (%)	0.89 (0.79 – 0.99)	> 30	87 (68 – 96)	67 (42 – 85)	2.6 (1.3 – 5.4)	0.20 (0.06 – 0.60)
LVSV-PuSV						
RV index (ml/m^2)	0.90 (0.80 – 1.0)	> 31	87 (68 – 96)	87 (62 – 96)	6.5 (1.8 – 23.9)	0.15 (0.05 – 0.44)
RF (%)	0.92 (0.82 – 1.0)	> 36	91 (73 – 98)	80 (55 – 93)	4.6 (1.7 – 12.7)	0.11 (0.03 – 0.42)

AoFlow, aortic flow; AUC, area under the curve; CI, confidence interval; EDV, end-diastolic volume; LVSV, left ventricular stroke volume; NLR, negative likelihood ratio; PLR, positive likelihood ratio; PuSV, pulmonary stroke volume; RF, regurgitant fraction; RV, regurgitant volume

Table 7 – Diagnostic performance of thresholds indicating hemodynamically significant chronic mitral regurgitation benefiting from surgery

	AUC (95% CI)	**Threshold**	**Sensitivity** (95% CI)	**Specificity** (95% CI)	**PLR** (95% CI)	**NLR** (95% CI)
EDV index (ml/m^2)	0.96 (0.91 – 1.0)	> 120	92 (75 – 98)	93 (70 – 99)	13.8 (2.1 – 92.0)	0.09 (0.02 – 0.33)
LAA index (cm^2/m^2)	0.88 (0.78 – 0.98)	> 15	84 (65 – 94)	73 (48 – 89)	3.2 (1.3 – 7.4)	0.22 (0.08 – 0.56)
LVSV-AoFF						
RV index (ml/m^2)	0.98 (0.96 – 1.0)	> 32	96 (81 – 99)	80 (55 – 93)	4.8 (1.7 – 13.3)	0.05 (0.01 – 0.35)
RF (%)	0.92 (0.82 – 1.0)	> 41	96 (81 – 99)	80 (55 – 93)	4.8 (1.7 – 13.3)	0.05 (0.01 – 0.35)
MiIF-AoFF						
RV index (ml/m^2)	1.0 (1.0 – 1.0)	> 20	100 (87 – 100)	100 (80 – 100)	-	-
RF (%)	0.99 (0.97 – 1.0)	> 30	96 (81 – 99)	93 (70 – 99)	14.4 (2.2 – 95.8)	0.04 (0.01 – 0.29)

AoFF, aortic forward flow; AUC, area under the curve; CI, confidence interval; EDV, end-diastolic volume; LAA, left atrial area; LVSV, left ventricular stroke volume; MiIF, mitral inflow; NLR, negative likelihood ratio; PLR, positive likelihood ratio; RF, regurgitant fraction; RV, regurgitant volume

5 DISCUSSION

5.1 Echocardiographic LV volumes can support the diagnosis of severe chronic AR or MR (Paper I)

In paper I, our findings indicate that both 2DE and RT3DE LV volumetric dimensions can support the diagnosis of severe chronic AR and MR, in contrast to the LV linear dimensions. Our proposed threshold values are based on a novel study design, which used CMR as reference to determine the true degree of LV dilatation in patients with hemodynamically significant regurgitation and proven surgical benefit.

As previously mentioned, the quantification of LV size and function is an essential part of the evaluation and management of patients with VHD (5,6,54-56). Current guidelines define the upper normal limits for LV linear and volumetric dimensions obtained by 2DE as well as RT3DE, and these thresholds are useful to support the presence of a mild regurgitation, but cannot be used to distinguish between moderate and severe regurgitation (54-56,85,86). Furthermore, current guidelines refer to LV linear dimensions indicating severe LV dilation with poor prognosis (5,6), but contain otherwise no reference values concerning LV dimensions that can further aid in the diagnosis of severe AR or MR. Our results demonstrate that echocardiographic LV linear dimensions are only moderately related to LV volumes obtained by CMR. This is in accordance with previous findings looking at the agreement between LV linear and volumetric dimensions both obtained by CMR (104).

This implies that the sole assessment of the one-dimensional LV linear dimensions as a marker of LV enlargement, which is a three-dimensional process, can lead to underestimation of the true regurgitation severity, as the true extent of LV dilatation is not captured. Therefore, LV volumetric dimensions are preferable to linear dimensions, as our results indicate. Currently, echocardiographic grading of regurgitation severity is based on an “integrative approach” combining results from several qualitative, semi-quantitative and quantitative parameters (54-56). Eccentric jets are a frequent finding in patients undergoing both aortic and mitral valve surgery due to a bicuspid valve (AR) or degenerative valve disease (MR), which implies problems for the standard echocardiographic parameters used for the grading of regurgitation severity. In these cases, the echocardiographic diagnosis is challenging due to fewer diagnostically reliable parameters, as the vena contracta is difficult to measure, the flow convergence zone is not hemispheric and the continuous Doppler signal is suboptimal due to incorrect alignment between the flow and ultrasound beam direction. Consequently, grading of regurgitation severity is often inconclusive or incongruent. In this context, the assessment of LV dilatation, as an additional marker, becomes even more important and might aid in the clinical decision-making, especially in cases of uncertainty. Severe chronic AR and MR cause marked LV dilatation and this finding strongly supports the diagnosis of severe regurgitation, as our data illustrates. Importantly, other causes of LV enlargement have to be considered especially in patients with reduced systolic function. Consequently, LV volumes as a supportive sign in the grading of regurgitation severity should be interpreted with caution if other relevant causes contributing to LV dilatation and/or reduced systolic function (LVEF < 50%) are present,

for instance ischemic heart disease. Since chronic AR is characterized by a combined volume and pressure overload, in contrast to pure volume overload in chronic MR, we observed also a difference in the LV remodeling process, with significantly larger EDVs in patients with AR. This was also the reason why we determined separate thresholds for both AR and MR.

The assessment of LVEF is important in patients with severe chronic regurgitation, especially among those who are asymptomatic. Our results show that only the LVEF from 2DE data showed a moderate agreement with CMR. In contrast, the LVEF based on either LV linear dimensions or RT3DE data significantly underestimated the LVEF in comparison with CMR and the agreement was poor. This suggests that the threshold to perform CMR should be low in asymptomatic patients to facilitate correct clinical decision-making and timing of surgery. Although serial assessment of LV dimensions and LVEF is best performed using CMR, the differences in reproducibility between 2DE, RT3DE and CMR are not large (data only shown in the manuscript). Thus, we suggest that in clinical practice the serial evaluation using 2DE or RT3DE should be sufficient in most cases and that the role of CMR for serial evaluation can be limited to patients with suboptimal echocardiographic image quality.

Study limitations

CMR provides currently the most exact assessment of LV volumes. Nonetheless, the method has several limitations, discussed in detail in the following sections 5.2 and 5.3, which might explaining some of the observed differences between the modalities.

The recent 2015 guidelines on “Cardiac Chamber Quantification” recommend for the assessment of LV volumes by both 2DE and

RT3DE, to delineate the endocardial border between the trabeculae and the compact myocardium (105). This will, as we have shown in paper II (106), reduce the differences between 2DE and RT3DE LV volumes, but we were hesitant to do so in this study as this border is difficult to identify and the method is still poorly described in the literature as well as in the current guidelines. Therefore, in order to maintain high reproducibility, we used the old 2DE definition of the endocardial border, where the trabeculae are excluded from the LV cavity (85). Furthermore, it should be kept in mind that so far no reference values exits for the new delineation method of the endocardial border for LV dimensions obtained by 2DE.

5.2 The main cause of echocardiographic underestimation of LV dimensions (Paper II)

In the second paper, we systematically analyzed the ability of 2DE, RT3DE and CMR to delineate dimensions with increasing complexity (diameter – area – volume) in a multimodality phantom model, as well as *in vivo*. Using this study design, we hoped to gain a clearer picture of the main cause of echocardiographic underestimation by assuming that the simplest one-dimensional parameters, like diameter, are influenced to a lesser degree by interfering factors than the more complex two- and three-dimensional parameters, like area and volume.

Our *in vivo* results show that the smallest degree of underestimation between 2DE and CMR existed for the LV end-diastolic linear dimensions in the SA projection due to a good detail in the echocardiographic image that enabled a sufficient differentiation

between trabeculated and compact myocardium. An even clearer differentiation was possible in end-systole, leading to an only small and non-significant difference between the modalities. We found similar results for the areal dimensions in SA, although the degree of underestimation increased for the end-diastolic dimensions. Interestingly, the degree of underestimation by RT3DE, when analyzing the linear and areal LV dimensions in SA, was significantly larger than for 2DE. The most likely explanation for this is that RT3DE SA projections were reconstructed by post-processing a data set acquired from the apical window. In general, projections that were acquired from the apical window had often a lower image detail in certain areas of the heart (especially the lateral wall in the 4CH and the anterior wall in the two-chamber view) than images obtained from the parasternal window. This resulted in an inferior ability to differentiate between trabeculated and compact myocardium, and consequently in a higher degree of underestimation. This is clearly illustrated by the 95% limits of agreement that were narrow for the SA-EDD and wide for the 4CH-EDD. As initially postulated, increased the degree of underestimation successively from linear to areal, and finally volumetric LV dimensions. When analyzed according to the same principles, 2DE and RT3DE determined similar LV volumes. This stands in clear contrast to previous studies, which showed significantly larger volumes for RT3DE than for 2DE (61,63). The main reason for this discrepancy is most likely due to differences in the endocardial border definition. According to guidelines, only the papillary muscles are included in the LV cavity for 2DE (85), whereas, in RT3DE, as in CMR, both the trabeculae and the papillary muscles are included in the LV cavity (86). When applying these guideline recommendations, our results were once again in agreement with

previous studies and the results from paper I. Furthermore, the close agreement between the 2DE and RT3DE results enable us to conclude that the presumed limitation of 2DE, using geometrical assumptions to calculate LV volumes according to the biplane method of disks, did not play an essential role in our study population as most of the hearts retained their symmetry. However, in the presence of irregular LV shapes and/or regional wall motion abnormalities geometrical assumptions can contribute to the differences between 2DE and RT3DE (70). Altogether, our findings clearly indicate that the underestimation of LV dimensions by 2DE and RT3DE in comparison with CMR is mainly due to inherent technical differences in the ability to differentiate trabeculated from compact myocardium. Using a different approach, Mor-Avi et al. (72) came to a similar conclusion, which was based on the observation that the exclusion of trabeculae from the LV cavity during volumetric analysis of interpolated 3D CMR data sets improved the agreement between RT3DE and CMR in a small number of patients. Taken together, these findings clearly indicate that heterogeneous criteria for endocardial border definition are an additional contributor to the differences between the modalities. Consequently, a uniform endocardial border definition is desirable and a prerequisite for comparisons across modalities. Therefore, to minimize the inter-modality discrepancies and to improve the accuracy of the most widely used imaging method for LV assessment, namely echocardiography, we advocate that both the papillary muscles and trabeculae should be included in the LV cavity for the assessment of all LV dimensions for all modalities.

Interestingly, the latest version of the echocardiographic guidelines on “Cardiac Chamber Quantification”, which have been published after this paper was initially submitted for publication, state

that for both 2DE and RT3DE the “volumetric measurements are usually based on tracings of the interface between the compacted myocardium and the LV cavity” (105). Concerning LV linear dimensions, the guidelines state that they should be delineated “on the interface between the myocardial wall and cavity” (105). These statements are still quite vague and a clear definition of how to identify the endocardial border on echocardiographic images is once again missing, most likely due to the lack of sufficient studies in this area. Therefore, further studies are needed to clearly define the endocardial border in a sufficient and reproducible way.

Using the current phantom study, it was possible to rule out calibration errors by the imaging and analysis systems as a reason for echocardiographic underestimation, and previous results were thereby supported (72). Nonetheless, additional factors, apart from those previously discussed, could have contributed to the discrepancy between the modalities. Much attention was paid to assure high image quality, equivalent measurement positions and to avoid LV foreshortening as well as off-axis views, factors we sought to minimize by using experienced examiners. One known problem when it comes to CMR is the tendency towards LV volume overestimation due to insufficient compensation for basal through-plane motion, an error we tried to minimize using a method previously described by Alfakih et al. (97). Furthermore, small differences in the endocardial border position can have significant effects on the determined dimensions (72), a factor we sought to minimize by using experienced examiners and clear criteria for the delineation of the endocardial border.

Underlying physical principles

In the following section, we will take a closer look at the underlying

physical principles, which determine the detail in an image, and will speculate on how they might further explain our findings:

The detail in an image, which enables a clear differentiation between trabeculated and compact myocardium, is determined by the spatial resolution, contrast and noise of the respective imaging modality.

Spatial resolution in echocardiography is determined by components in three directions: axial, lateral and elevational resolution (107-109). In CMR, on the other hand, spatial resolution is determined by the slice thickness and image matrix that in turn is dependant on the number of frequency-encoded and phase-encoded projections for a given field of view (110-113). It is known that echocardiography, in comparison with CMR, has a better or similar in-plane spatial resolution in the axial and at the focus position of the lateral direction. Nonetheless, the depth-dependant lateral resolution, which is overall inferior to the axial resolution, might lead to fusion of trabeculae with compact myocardium, as they can no longer be sufficiently separated as individual structures, especially in certain regions of the near and far field of the ultrasound beam. Interestingly, despite a superior axial resolution, our 2DE and RT3DE results depicted the LV as significantly shorter in comparison with CMR (data not included in the published article). This is in accordance with previous findings by Jenkins et al. (114). The simplest explanation would be LV foreshortening due to improper image alignment by 2DE and RT3DE, although much care was taken to avoid this. A further more likely cause for this discrepancy is the occurrence of apical trabeculations, which cannot be delineated sufficiently as separate structures. Even the fact that lateral resolution is poorer in the near field close to the transducer surface and that the usage of tissue harmonic imaging

improves lateral resolution but reduces axial resolution has to be taken into account as possible contributing causes (115). An additional factor that can impair the lateral resolution in echocardiography is a reduced scan line density, for instance due to a large scan volume in RT3DE, as in patients with valvular heart disease (116).

Contrast in echocardiography depends on the difference in acoustic impedance and attenuation of adjacent tissues/materials as well as spatial resolution (107-109). In CMR, on the other hand, contrast is determined by the type of pulse sequence, difference in T1 and T2 relaxation times and proton density of adjacent tissues (110-113). The currently most widely used balanced steady-state free precession sequences for LV assessment depend for their signal on the square root of the T2/T1 ratio and the proton density, thus providing a good contrast between blood and adjacent myocardium (117). In contrast, older spoiled gradient-echo sequences with their poorer contrast and thereby poorer visualization of the endocardial border lead to significantly smaller LV volumes (118). Under optimal conditions, as illustrated by our phantom results, echocardiography can in the presence of sufficient contrast delineate dimensions with similar precision as CMR apart from the effect of a depth-dependant lateral resolution. During the echocardiographic exam of the phantom model good contrast was provided due to a high difference in acoustic impedance and attenuation between water with added potato flower (~1.48 x 10^6 kg/(m^2s) and ~0.0002 (dB/cm)/MHz respectively) and polycarbonate (~2.69 x 10^6 kg/(m^2s) and ~4.98 (dB/cm)/MHz respectively) as well as a specular reflector in form of a smooth surface providing a good signal-to-noise ratio and thereby a good contrast-to-noise ratio. In contrast, *in vivo* the difference in acoustic

impedance and attenuation between blood (~1.65 x 10^6 kg/(m^2s) and ~0.18 (dB/cm)/MHz respectively) and myocardium (~1.71 x 10^6 kg/(m^2s) and ~0.5 (dB/cm)/MHz respectively) is much smaller and the trabeculations with their irregular surface provide a non-specular reflector, which in turn results in more attenuation due to scattering and thereby to a poorer signal-to-noise ratio and contrast-to-noise ratio. Another factor contributing to a poorer signal-to-noise ratio and contrast-to-noise ratio is the non-perpendicular incidence of ultrasound waves with tissue boundaries in certain areas of the heart, especially when using images obtained from the apical window. It is known that CMR has a superior image contrast compared with echocardiography even when adding ultrasound contrast. Nonetheless, the application of ultrasound contrast can lead to an improvement in the endocardial border definition and is a potential solution to improve the echocardiographic contrast (114,119).

Further studies are needed to clarify the exact effect of the differences in spatial resolution, contrast and noise, as well as their determinants, as the possible underlying main cause of the underestimation of LV dimensions by 2DE and RT3DE in comparison with CMR.

Study limitations

Importantly, the study has to cope with a sampling bias as patients with a severely dilated LV had more frequently a 2DE and RT3DE data set that did not fulfill our strict analysis criteria. Since the extent of underestimation increases with the severity of LV dilatation (120), it is most likely that in reality the degree of echocardiographic underestimation is larger than reported in paper II.

5.3 The choice of CMR quantification method can affect the grading of MR severity (Paper III)

In paper III, we systematically compared three different CMR methods for indirect MR quantification. In healthy volunteers without MR, our results showed a clear tendency of the 'standard' method towards LVSV overestimation resulting, accordingly, in larger RVs and RFs in patients with MR, in contrast to the 'volumetric' and 'flow' method, which determined similar results. Consequently, the choice of method can affect the grading of MR severity. Inter-observer variability was lowest for the 'flow' and highest for the 'volumetric' method, while intra-observer variability was similar for all three methods.

Each indirect method uses either the slice summation technique and/or PC imaging, solely or in combination, for MR quantification. The slice summation technique provides currently the most exact ventricular volumes, nonetheless, has the technique certain limitations. The inclusion or exclusion of the papillary muscles and trabeculae in the ventricular cavity affect the determined ventricular volumes significantly (121). In the current study, we included both the papillary muscles and trabeculae in the ventricular cavity, a technique often used in clinical practice due to its good reproducibility, which leads, nonetheless, to larger EDVs, ESVs and SVs (122). Furthermore, inconsistent inclusion in end-diastole and unintentional exclusion of trabeculae in end-systole, as the differentiation between compact and trabeculated myocardium becomes more difficult, can lead to overestimation of the determined SV. Another factor influencing the determined ESV and SV is the phenomenon of through-plane motion of the basal slice (73), an error we aimed to minimize using a method previously described by Alfakih et al (97).

This method, although easy to apply and widely used, is not entirely correct since it does not take the left ventricular outflow tract and the shape of the mitral valve into account. Furthermore, accurate differentiation between the left ventricle and left atrium is difficult due to a partial volume effect. Altogether, these factors are most likely the explanation for the in the study observed tendency of the 'standard' method towards LVSV overestimation resulting, consequently, in larger RVs and RFs in patients with MR. PC imaging, on the other hand, allows accurate quantification of cardiac blood flow (90,123), and has been shown to correspond well to Doppler echocardiography as well as fair to invasive techniques (123,124). Nonetheless, PC imaging has in general to cope with certain pitfalls and limitations as caused by mismatch of the encoding velocity, misalignment of the image plane, inadequate temporal resolution, inadequate spatial resolution/partial volume effects, accelerated flow, spatial misregistrations, signal loss and/or BPEs (90,98,125). We aimed, as previously described in the methods section, to minimize these pitfalls and limitations among others through accurate alignment and positioning of the imaging slice, setting of an adjusted VENC and correction for BPEs (90). Furthermore, it has previously been shown that the position of the imaging slice in the aortic as well as the mitral position is important for flow quantification by CMR (79,90,126). In accordance with previous recommendations, the AoFF was determined at the level of the sinutubular junction (90). To quantify the MiIF, we chose an imaging slice position approximately 1 cm below the mitral annulus (ventricular side), which can, according to previous results, lead to a significantly smaller MiIF in comparison to the mitral annulus position (79). This might have contributed to a slight underestimation of the MiIF and thereby MRVs, but according to our

own experience, the chosen method provided more reproducible measurements (results not shown). The motion of the aortic and mitral valve is a further complicating factor of PC imaging since it interferes with the appropriate positioning of the imaging slice. Moving slice PC imaging has been developed to overcome this problem, a method that determined considerably larger MRFs than without correction (127). This is a highly complex technique with limited availability. Nonetheless, we have tested this technique at our institution but were not convinced of its applicability.

Previous studies reported smaller differences when comparing the ‘standard’ versus the ‘volumetric’ method (80,81). Nonetheless, a direct comparison with our results is difficult as both studies used either gradient echo sequences to obtain ventricular volumes, resulting in smaller volumes, or different analysis tools, which exclude the papillary muscles from the ventricular cavity and use a different approach for basal through-plane motion compensation. PC imaging has, as shown by our results and in accordance with previous findings, a lower inter- and intra-observer variability than the slice summation technique as well as a low variability for repeated measurements (97,123). As a consequence, we observed, in accordance with previous studies, the lowest variability for the ‘flow’ and the highest variability for the ‘volumetric’ method as it uses the slice summation technique twice (79,81). A major limitation of the ‘volumetric’ method is concomitant tricuspid regurgitation, a common finding in MR patients, as the method can only be applied in the absence of multivalvular disease and intra-cardiac shunt. This makes the ‘volumetric’ method, together with its high variability, to the least favorable of the three methods.

In a subgroup of operated patients with severe MR, we were able to show that the choice of method can affect the grading of MR severity and thereby eventually the clinical decision-making and timing of surgery. Furthermore, the RVs were, irrespective of the chosen method, in most cases above the guideline threshold of ≥ 60 ml, while the RFs were more frequently below the threshold of ≥ 50% (5). Consequently, diagnostic incongruence between the calculated RV and RF was a frequent finding in this study. Hereby should be kept in mind that a certain degree of diagnostic incongruence will merely occur due to patients that lie just above or below the respective threshold. These findings clearly indicate, in accordance with previous studies (83,84), that CMR-specific thresholds for severe regurgitation might differ from recognized guideline cut-off values. This was further investigated in the fourth paper of this thesis.

Study limitations

A limiting factor, as for all other studies investigating the diagnostic accuracy for MR quantification, is the lack of a true “gold standard”. Therefore, it is difficult to say, which method is the most accurate and reliable. Nonetheless, healthy volunteers without MR were included in the study design as a control group and uncovered a clear tendency of the ‘standard’ method towards LVSV overestimation.

5.4 CMR grading thresholds indicating hemodynamically significant AR or MR (Paper IV)

In the fourth paper, the application of current guideline RF thresholds led to frequently discordant grading between 2DE and CMR.

Furthermore, we were able to determine quantification method-specific thresholds for CMR RV indices and RFs indicating hemodynamically significant chronic AR or MR benefiting from surgery, which are lower than the recognized guideline criteria. Furthermore, we provide thresholds for EDV indices supporting the diagnosis of hemodynamically significant chronic regurgitation.

As previously mentioned, accurate grading of regurgitation severity is of utmost clinical importance, but one of the most difficult problems in valvular heart disease. Currently, CMR grading of AR and MR severity is usually based on the same thresholds as echocardiography, which were originally defined through the calibration of quantitative Doppler echocardiography against angiographic grading of regurgitation severity (54,68). However, angiographic grading itself has several limitations and is, nowadays, considered inferior to echocardiography. Furthermore, the relation between quantitative Doppler echocardiography and CMR has only been studied in a small number of patients, of which even fewer patients fulfilled the criteria for severe regurgitation (78,128). Consequently, the approach to identify CMR-specific thresholds by using another modality as reference is difficult, since each reference method has its own limitations. To avoid this drawback, we used patients with proven hemodynamically significant regurgitation and surgical benefit as reference, defined by a post-surgical reduction in EDV index of ≥ 15% and/or relief of symptoms. Clearly, the hypothesis that post-surgical reverse remodeling and/or relief of symptoms are solely related to the surgical correction of valvular regurgitation is an oversimplification, but in the context of previous studies a reasonable approximation (24,129). Nonetheless, several other factors could have

contributed as well, as changes in medication or physical activity or cardiac rhythm.

Our determined quantification method-specific CMR RF thresholds indicating hemodynamically significant chronic AR or MR benefiting from surgery were lower than the recognized guideline thresholds for severe regurgitation (5). No comparison was possible concerning RV indices, as no reference values are reported in current guidelines. Our identified CMR-specific thresholds are in keeping with two previous studies on chronic AR, which used two completely different study designs. The first study by Myerson et al. (84), looking for the link between clinical outcome and CMR grading of regurgitation severity, identified several quantitative parameters, which were associated with the development of symptoms and/or progression to surgery, including a RV index > 23 ml/m^2 and RF > 33% using the direct quantification method. The second study by Gabriel et al. (83), looking for the best concordance between echocardiographic and CMR grading of regurgitation severity, identified a RF > 30% as threshold for severe regurgitation when using the direct quantification method. In contrast to our and previous findings, stands a third study on AR and MR by Gelfand et al. (82), which looked once again for the best concordance between echocardiographic and CMR grading of regurgitation severity. This study identified a RF > 48% as threshold for both severe AR and MR, using direct quantification for AR and indirect quantification (LVSV-AoFF) for MR respectively.

The clear quantification method-dependence of both AR and MR grading is in accordance with our previous findings in MR patients (Paper III) (130). In general, methods using a combination of PC imaging and the slice summation technique determined in both AR and MR larger RV indices and RFs than methods using solely PC

imaging. Possible explanations for these observed differences are the tendency of the slice summation technique towards LVSV overestimation, the potential for underestimation of AoFF and PuSV using PC imaging or both (discussed in detail in the previous section 5.3). Interestingly, the obtained thresholds indicating severe AR and MR were identical for quantification methods using solely PC imaging and similar for quantification methods using a combination of PC imaging and slice summation technique. This finding is in accordance with current guidelines and the previously mentioned study by Gelfand et al. (82).

Furthermore, our findings indicate that the application of current guideline RF thresholds leads in operated patients with severe AR or MR, as determined by 2DE, to frequently discordant grading as moderate or even mild regurgitation by CMR. A finding, which is in agreement with recent results in patients with MR by Uretsky et al. (129). Since CMR is often used as a second line diagnostic tool in cases of echocardiographic uncertainty, this downgrading by CMR can potentially delay surgery in patients that otherwise would benefit from intervention.

Our results show that the EDV index, as indicator of the degree of LV remodeling, can be of additive value supporting the diagnosis of hemodynamically significant regurgitation. This expands the current diagnostic arsenal and may especially be useful in cases of diagnostic uncertainty. Importantly, other causes of LV dilation have to be excluded prior to the application of this parameter, especially in patients with LV systolic dysfunction. This is in accordance with our findings in paper I and a previous CMR study, which identified in patients with AR an EDV index > 129 ml/m^2 as threshold associated with poorer prognosis (84).

Study limitations

The relatively small number of highly selected patients limits the strength of our conclusions as well as the general applicability of the obtained thresholds. This is of special importance in the group of patients with severe MR, which had in relation to patients with moderate regurgitation, clearly larger RV indices and RFs. Although both groups had degenerative disease with prolapse (apart from one patient), it is conceivable that an additional chordae rupture will worsen the degree of regurgitation significantly, resulting in a clear distinction between moderate and severe MR. Consequently, our MR thresholds should be interpreted with caution and not extrapolated to patients with functional MR. However, our findings are of clinical relevance as the majority of MR patients undergoing surgery have, nowadays, degenerative disease with prolapse. In the present study, special care was taken to assure high accuracy of PC imaging. Nonetheless, several factors could have contributed to eventual underestimation of the quantified flow: valvular motion, choice of slice positioning and altered flow patterns due to a bicuspid aortic valve or dilated ascending aorta (90,126,131-134). Consequently, the highest risk for underestimation exists for the direct AR quantification method.

6 CONCLUSIONS

- We propose 2DE and RT3DE thresholds for LV volumes indicating severe chronic AR or MR, which can support the diagnosis of severe chronic regurgitation. Importantly, prior to the application of these thresholds, other causes for LV enlargement have to be considered, especially in patients with reduced LVEF. Furthermore, LV volumetric dimensions are superior to linear dimensions in the assessment of LV dilatation, and 2DE is still more feasible and superior to RT3DE in the assessment of LV volumes and systolic function in this patient group.

- Underestimation of LV dimensions by 2DE and RT3DE compared with CMR is mainly due to inherent technical differences in the ability to differentiate trabeculated from compact myocardium. Identical endocardial border definition criteria are needed to minimize differences between the modalities and to ensure better comparability in clinical practice.

- In healthy volunteers without MR, the ‘standard’ method shows a clear tendency towards LVSV overestimation resulting, accordingly, in larger RVs and RFs in patients with MR, in contrast to the ‘volumetric’ and ‘flow’ method, which determine similar MR quantification results. Consequently, the choice of

method can affect the grading of MR severity and thereby eventually the clinical decision-making and timing of surgery.

- CMR grading of chronic AR and MR severity based on current guideline criteria leads to frequent downgrading compared with 2DE. Furthermore, our findings indicate that CMR grading of chronic AR and MR should be based on modality- and quantification method-specific thresholds, as they differ from recognized guideline criteria and are dependant on the quantification method used, to assure appropriate clinical decision-making and timing of surgery. Finally, we propose CMR- and quantification method-specific thresholds indicating hemodynamically significant AR or MR benefiting from surgery.

FUTURE PERSPECTIVES

Much remains to be done in the field of VHD, both from a clinical as well as diagnostic perspective. Focusing on the diagnosis using non-invasive imaging techniques, the spectrum of remaining problems is rather broad, as highlighted by our research, ranging from basic methodological problems to more complex multi-parametric analysis approaches. To improve the most important diagnostic challenge, namely the grading of regurgitation severity, we need a better understanding of the natural history of VHD and continue our search for new diagnostic parameters as well as techniques. Hereby, we should not only focus on the diseased valve itself, but also on the resulting altered flow patterns, remodeling processes and systemic effects. A multi-parametric grading approach, looking at different aspects of the disease, will most likely hold the key to success. To achieve this, further studies are needed to find the right combination of already existing as well as new diagnostic parameters that take not only different imaging parameters into account but also biochemical and molecular markers.

ACKNOWLEDGEMENTS

I wish to express my sincere gratitude to all those who contributed to this thesis. In particular I would like to thank:

My main supervisor, **Odd Bech-Hanssen**, for his enthusiasm, never-ending support and introduction to research in the field of cardiovascular imaging.

My co-supervisor, **Kerstin Lagerstrand**, for her passion, companionship during long scan hours and interesting discussions about the physics of medical imaging.

My co-supervisor, **Åse Johnsson**, for her unrestricted support, constructive criticism of my research and introduction to cardio-vascular imaging.

My college, **Sinsia Gao**, for her dedicated help with echocardiography and constructive criticism of my research.

My college, **Carl Lamm**, for his encouragement and opening of many doors, which made my start in cardiovascular magnetic resonance imaging at the Sahlgrenska University Hospital possible.

The present and former heads of the Department of Cardiology, **Per Albertsson**, **Göran Matejka** and **Lars Grip**, for enabling this thesis as well as their courage and long-sightedness in training a young cardiologist in multimodality cardiovascular imaging.

My co-workers, **Sofia Lindbom** and **Lena Johansson**, for their help with echocardiography, as well as **Jakobína Grétarsdottír** and **Jan Samuelsson**, for enabling the building and final construction of the multimodality phantom model.

All my colleagues/co-workers of the **Departments of Cardiology**, **Clinical Physiology**, **Radiology**, **Diagnostic Radiation Physics** and **Thoracic Surgery** for a great working atmosphere and unparalleled cross-disciplinary cooperation.

My colleague and friend, **Georg Haltern**, for introducing me to cardiovascular imaging, giving my career a clear direction.

My family, **Christina Polte**, **Malin Polte** and **Isis Polte-Schwarz**, for all their understanding and support through all my life.

FUNDING

The research of this thesis was funded by a project grant from the Health & Medical Care Committee of the Regional Executive Board (Grant no: 100431), Västra Götaland Region and by a “Hjärtfondens forskningsstipendium 2015”.

REFERENCES

1. Nkomo VT, Gardin JM, Skelton TN, Gottdiener JS, Scott CG, Enriquez-Sarano M. Burden of valvular heart diseases: a population-based study. Lancet 2006;368:1005-11.
2. Iung B, Baron G, Butchart EG, et al. A prospective survey of patients with valvular heart disease in Europe: The Euro Heart Survey on Valvular Heart Disease. Eur Heart J 2003;24:1231-43.
3. Klein AL, Burstow DJ, Tajik AJ, et al. Age-related prevalence of valvular regurgitation in normal subjects: a comprehensive color flow examination of 118 volunteers. J Am Soc Echocardiogr 1990;3:54-63.
4. Soler-Soler J, Galve E. Worldwide perspective of valve disease. Heart 2000;83:721-5.
5. Nishimura RA, Otto CM, Bonow RO, et al. 2014 AHA/ACC guideline for the management of patients with valvular heart disease: a report of the American College of Cardiology/American Heart Association Task Force on Practice Guidelines. J Am Coll Cardiol 2014;63:e57-185.
6. Vahanian A, Alfieri O, Andreotti F, et al. Guidelines on the management of valvular heart disease (version 2012). Eur Heart J 2012;33:2451-96.
7. Enriquez-Sarano M, Tajik AJ. Clinical practice. Aortic regurgitation. N Engl J Med 2004;351:1539-46.
8. Kang DH, Kim JH, Rim JH, et al. Comparison of early surgery versus conventional treatment in asymptomatic severe mitral regurgitation. Circulation 2009;119:797-804.
9. Enriquez-Sarano M, Avierinos JF, Messika-Zeitoun D, et al. Quantitative determinants of the outcome of asymptomatic mitral regurgitation. N Engl J Med 2005;352:875-83.
10. Enriquez-Sarano M, Sundt TM, 3rd. Early surgery is recommended for mitral regurgitation. Circulation 2010;121:804-11; discussion 812.
11. Mirabel M, Iung B, Baron G, et al. What are the characteristics of patients with severe, symptomatic, mitral regurgitation who are denied surgery? Eur Heart J 2007;28:1358-65.
12. Bach DS, Awais M, Gurm HS, Kohnstamm S. Failure of guideline adherence for intervention in patients with severe mitral regurgitation. J Am Coll Cardiol 2009;54:860-5.
13. Bonow RO, Otto CM. Valvular heart disease: a companion to Braunwald's heart disease. 4th ed: Elsevier, 2014.
14. Bonow RO, Mann DL, Zipes DP, Libby P. Braunwald's heart disease: a textbook of cardiovascular medicine. 9th ed: Elsevier, 2012.
15. Wang A, Bashore TM. Valvular heart disease. 1st ed: Humana Press, 2009.

16. Carabello BA. Aortic regurgitation. A lesion with similarities to both aortic stenosis and mitral regurgitation. Circulation 1990;82:1051-3.
17. Ross J, Jr. Afterload mismatch in aortic and mitral valve disease: implications for surgical therapy. J Am Coll Cardiol 1985;5:811-26.
18. Borow KM. Surgical outcome in chronic aortic regurgitation: a physiologic framework for assessing preoperative predictors. J Am Coll Cardiol 1987;10:1165-70.
19. Chaliki HP, Mohty D, Avierinos JF, et al. Outcomes after aortic valve replacement in patients with severe aortic regurgitation and markedly reduced left ventricular function. Circulation 2002;106:2687-93.
20. Goldschlager N, Pfeifer J, Cohn K, Popper R, Selzer A. The natural history of aortic regurgitation. A clinical and hemodynamic study. Am J Med 1973;54:577-88.
21. Dujardin KS, Enriquez-Sarano M, Schaff HV, Bailey KR, Seward JB, Tajik AJ. Mortality and morbidity of aortic regurgitation in clinical practice. A long-term follow-up study. Circulation 1999;99:1851-7.
22. Klodas E, Enriquez-Sarano M, Tajik AJ, Mullany CJ, Bailey KR, Seward JB. Optimizing timing of surgical correction in patients with severe aortic regurgitation: role of symptoms. J Am Coll Cardiol 1997;30:746-52.
23. Gaasch WH, Carroll JD, Levine HJ, Criscitiello MG. Chronic aortic regurgitation: prognostic value of left ventricular end-systolic dimension and end-diastolic radius/thickness ratio. J Am Coll Cardiol 1983;1:775-82.
24. Bonow RO, Dodd JT, Maron BJ, et al. Long-term serial changes in left ventricular function and reversal of ventricular dilatation after valve replacement for chronic aortic regurgitation. Circulation 1988;78:1108-20.
25. Bonow RO, Lakatos E, Maron BJ, Epstein SE. Serial long-term assessment of the natural history of asymptomatic patients with chronic aortic regurgitation and normal left ventricular systolic function. Circulation 1991;84:1625-35.
26. Tornos P, Sambola A, Permanyer-Miralda G, Evangelista A, Gomez Z, Soler-Soler J. Long-term outcome of surgically treated aortic regurgitation: influence of guideline adherence toward early surgery. J Am Coll Cardiol 2006;47:1012-7.
27. Freed LA, Levy D, Levine RA, et al. Prevalence and clinical outcome of mitral-valve prolapse. N Engl J Med 1999;341:1-7.
28. Disse S, Abergel E, Berrebi A, et al. Mapping of a first locus for autosomal dominant myxomatous mitral-valve prolapse to chromosome 16p11.2-p12.1. Am J Hum Genet 1999;65:1242-51.
29. Freed LA, Acierno JS, Jr., Dai D, et al. A locus for autosomal dominant mitral valve prolapse on chromosome 11p15.4. Am J Hum Genet 2003;72:1551-9.
30. Nesta F, Leyne M, Yosefy C, et al. New locus for autosomal dominant mitral valve prolapse on chromosome 13: clinical insights from genetic studies. Circulation 2005;112:2022-30.

31. Adams DH, Anyanwu AC. Seeking a higher standard for degenerative mitral valve repair: begin with etiology. J Thorac Cardiovasc Surg 2008;136:551-6.
32. Anyanwu AC, Adams DH. Etiologic classification of degenerative mitral valve disease: Barlow's disease and fibroelastic deficiency. Semin Thorac Cardiovasc Surg 2007;19:90-6.
33. Fornes P, Heudes D, Fuzellier JF, Tixier D, Bruneval P, Carpentier A. Correlation between clinical and histologic patterns of degenerative mitral valve insufficiency: a histomorphometric study of 130 excised segments. Cardiovasc Pathol 1999;8:81-92.
34. Adams DH, Rosenhek R, Falk V. Degenerative mitral valve regurgitation: best practice revolution. Eur Heart J 2010;31:1958-66.
35. Guy TS, Hill AC. Mitral valve prolapse. Annu Rev Med 2012;63:277-92.
36. Enriquez-Sarano M, Basmadjian AJ, Rossi A, Bailey KR, Seward JB, Tajik AJ. Progression of mitral regurgitation: a prospective Doppler echocardiographic study. J Am Coll Cardiol 1999;34:1137-44.
37. Devereux RB, Hawkins I, Kramer-Fox R, et al. Complications of mitral valve prolapse. Disproportionate occurrence in men and older patients. Am J Med 1986;81:751-8.
38. Avierinos JF, Inamo J, Grigioni F, Gersh B, Shub C, Enriquez-Sarano M. Sex differences in morphology and outcomes of mitral valve prolapse. Ann Intern Med 2008;149:787-95.
39. Duren DR, Becker AE, Dunning AJ. Long-term follow-up of idiopathic mitral valve prolapse in 300 patients: a prospective study. J Am Coll Cardiol 1988;11:42-7.
40. Tribouilloy CM, Enriquez-Sarano M, Schaff HV, et al. Impact of preoperative symptoms on survival after surgical correction of organic mitral regurgitation: rationale for optimizing surgical indications. Circulation 1999;99:400-5.
41. Ling LH, Enriquez-Sarano M, Seward JB, et al. Clinical outcome of mitral regurgitation due to flail leaflet. N Engl J Med 1996;335:1417-23.
42. Messika-Zeitoun D, Bellamy M, Avierinos JF, et al. Left atrial remodelling in mitral regurgitation--methodologic approach, physiological determinants, and outcome implications: a prospective quantitative Doppler-echocardiographic and electron beam-computed tomographic study. Eur Heart J 2007;28:1773-81.
43. Hammermeister KE, Fisher L, Kennedy W, Samuels S, Dodge HT. Prediction of late survival in patients with mitral valve disease from clinical, hemodynamic, and quantitative angiographic variables. Circulation 1978;57:341-9.
44. Grigioni F, Avierinos JF, Ling LH, et al. Atrial fibrillation complicating the course of degenerative mitral regurgitation: determinants and long-term outcome. J Am Coll Cardiol 2002;40:84-92.

45. Braunberger E, Deloche A, Berrebi A, et al. Very long-term results (more than 20 years) of valve repair with carpentier's techniques in nonrheumatic mitral valve insufficiency. Circulation 2001;104:I8-11.
46. Montant P, Chenot F, Robert A, et al. Long-term survival in asymptomatic patients with severe degenerative mitral regurgitation: a propensity score-based comparison between an early surgical strategy and a conservative treatment approach. J Thorac Cardiovasc Surg 2009;138:1339-48.
47. Baron MG. Angiocardiographic evaluation of valvular insufficiency. Circulation 1971;43:599-605.
48. Sandler H, Dodge HT, Hay RE, Rackley CE. Quantitation of valvular insufficiency in man by angiocardiography. Am Heart J 1963;65:501-13.
49. Hunt D, Baxley WA, Kennedy JW, Judge TP, Williams JE, Dodge HT. Quantitative evaluation of cineaortography in the assessment of aortic regurgitation. Am J Cardiol 1973;31:696-700.
50. Honey M, Gough JH, Katsaros S, Miller GA, Thuraisingham V. Left ventricular cine-angio- cardiography in the assessment of mitral regurgitation. Br Heart J 1969;31:596-602.
51. Lopez JF, Hanson S, Orchard RC, Tan L. Quantification of mitral valvular incompetence. Cathet Cardiovasc Diagn 1985;11:139-52.
52. Rokey R, Sterling LL, Zoghbi WA, et al. Determination of regurgitant fraction in isolated mitral or aortic regurgitation by pulsed Doppler two-dimensional echocardiography. J Am Coll Cardiol 1986;7:1273-8.
53. Hundley WG, Li HF, Willard JE, et al. Magnetic resonance imaging assessment of the severity of mitral regurgitation. Comparison with invasive techniques. Circulation 1995;92:1151-8.
54. Zoghbi WA, Enriquez-Sarano M, Foster E, et al. Recommendations for evaluation of the severity of native valvular regurgitation with two-dimensional and Doppler echocardiography. J Am Soc Echocardiogr 2003;16:777-802.
55. Lancellotti P, Tribouilloy C, Hagendorff A, et al. European Association of Echocardiography recommendations for the assessment of valvular regurgitation. Part 1: aortic and pulmonary regurgitation (native valve disease). Eur J Echocardiogr 2010;11:223-44.
56. Lancellotti P, Moura L, Pierard LA, et al. European Association of Echocardiography recommendations for the assessment of valvular regurgitation. Part 2: mitral and tricuspid regurgitation (native valve disease). Eur J Echocardiogr 2010;11:307-32.
57. Biner S, Rafique A, Rafii F, et al. Reproducibility of proximal isovelocity surface area, vena contracta, and regurgitant jet area for assessment of mitral regurgitation severity. JACC Cardiovasc Imaging 2010;3:235-43.
58. Dahiya A, Bolen M, Grimm RA, Rodriguez LL, Thomas JD, Marwick TH. Development of a consensus document to improve multireader

concordance and accuracy of aortic regurgitation severity grading by echocardiography versus cardiac magnetic resonance imaging. Am J Cardiol 2012;110:709-14.
59. Bellenger NG, Burgess MI, Ray SG, et al. Comparison of left ventricular ejection fraction and volumes in heart failure by echocardiography, radionuclide ventriculography and cardiovascular magnetic resonance: are they interchangeable? Eur Heart J 2000;21:1387-96.
60. Grothues F, Smith GC, Moon JC, et al. Comparison of interstudy reproducibility of cardiovascular magnetic resonance with two-dimensional echocardiography in normal subjects and in patients with heart failure or left ventricular hypertrophy. Am J Cardiol 2002;90:29-34.
61. Gutierrez-Chico JL, Zamorano JL, Perez de Isla L, et al. Comparison of left ventricular volumes and ejection fractions measured by three-dimensional echocardiography versus by two-dimensional echocardiography and cardiac magnetic resonance in patients with various cardiomyopathies. Am J Cardiol 2005;95:809-13.
62. Jenkins C, Bricknell K, Hanekom L, Marwick TH. Reproducibility and accuracy of echocardiographic measurements of left ventricular parameters using real-time three-dimensional echocardiography. J Am Coll Cardiol 2004;44:878-86.
63. Chuang ML, Hibberd MG, Salton CJ, et al. Importance of imaging method over imaging modality in noninvasive determination of left ventricular volumes and ejection fraction: assessment by two- and three-dimensional echocardiography and magnetic resonance imaging. J Am Coll Cardiol 2000;35:477-84.
64. Dorosz JL, Lezotte DC, Weitzenkamp DA, Allen LA, Salcedo EE. Performance of 3-dimensional echocardiography in measuring left ventricular volumes and ejection fraction: a systematic review and meta-analysis. J Am Coll Cardiol 2012;59:1799-808.
65. Longmore DB, Underwood SR, Hounsfield GN, et al. Dimensional accuracy of magnetic resonance in studies of the heart. Lancet 1985;1:1360-2.
66. Rehr RB, Malloy CR, Filipchuk NG, Peshock RM. Left ventricular volumes measured by MR imaging. Radiology 1985;156:717-9.
67. Tribouilloy CM, Enriquez-Sarano M, Bailey KR, Seward JB, Tajik AJ. Assessment of severity of aortic regurgitation using the width of the vena contracta: A clinical color Doppler imaging study. Circulation 2000;102:558-64.
68. Dujardin KS, Enriquez-Sarano M, Bailey KR, Nishimura RA, Seward JB, Tajik AJ. Grading of mitral regurgitation by quantitative Doppler echocardiography: calibration by left ventricular angiography in routine clinical practice. Circulation 1997;96:3409-15.
69. King DL, Harrison MR, King DL, Jr., Gopal AS, Kwan OL, DeMaria AN. Ultrasound beam orientation during standard two-dimensional

imaging: assessment by three-dimensional echocardiography. J Am Soc Echocardiogr 1992;5:569-76.
70. Chukwu EO, Barasch E, Mihalatos DG, et al. Relative importance of errors in left ventricular quantitation by two-dimensional echocardiography: insights from three-dimensional echocardiography and cardiac magnetic resonance imaging. J Am Soc Echocardiogr 2008;21:990-7.
71. Miller CA, Pearce K, Jordan P, et al. Comparison of real-time three-dimensional echocardiography with cardiovascular magnetic resonance for left ventricular volumetric assessment in unselected patients. Eur Heart J Cardiovasc Imaging 2012;13:187-95.
72. Mor-Avi V, Jenkins C, Kuhl HP, et al. Real-time 3-dimensional echocardiographic quantification of left ventricular volumes: multicenter study for validation with magnetic resonance imaging and investigation of sources of error. JACC Cardiovasc Imaging 2008;1:413-23.
73. Marcus JT, Gotte MJ, DeWaal LK, et al. The influence of through-plane motion on left ventricular volumes measured by magnetic resonance imaging: implications for image acquisition and analysis. J Cardiovasc Magn Reson 1999;1:1-6.
74. Myerson SG. Heart valve disease: investigation by cardiovascular magnetic resonance. J Cardiovasc Magn Reson 2012;14:7.
75. Cawley PJ, Maki JH, Otto CM. Cardiovascular magnetic resonance imaging for valvular heart disease: technique and validation. Circulation 2009;119:468-78.
76. Chan KM, Wage R, Symmonds K, et al. Towards comprehensive assessment of mitral regurgitation using cardiovascular magnetic resonance. J Cardiovasc Magn Reson 2008;10:61.
77. Honda N, Machida K, Hashimoto M, et al. Aortic regurgitation: quantitation with MR imaging velocity mapping. Radiology 1993;186:189-94.
78. Kizilbash AM, Hundley WG, Willett DL, Franco F, Peshock RM, Grayburn PA. Comparison of quantitative Doppler with magnetic resonance imaging for assessment of the severity of mitral regurgitation. Am J Cardiol 1998;81:792-5.
79. Fujita N, Chazouilleres AF, Hartiala JJ, et al. Quantification of mitral regurgitation by velocity-encoded cine nuclear magnetic resonance imaging. J Am Coll Cardiol 1994;23:951-8.
80. Myerson SG, Francis JM, Neubauer S. Direct and indirect quantification of mitral regurgitation with cardiovascular magnetic resonance, and the effect of heart rate variability. MAGMA 2010;23:243-9.
81. Kon MW, Myerson SG, Moat NE, Pennell DJ. Quantification of regurgitant fraction in mitral regurgitation by cardiovascular magnetic resonance: comparison of techniques. J Heart Valve Dis 2004;13:600-7.

82. Gelfand EV, Hughes S, Hauser TH, et al. Severity of mitral and aortic regurgitation as assessed by cardiovascular magnetic resonance: optimizing correlation with Doppler echocardiography. J Cardiovasc Magn Reson 2006;8:503-7.
83. Gabriel RS, Renapurkar R, Bolen MA, et al. Comparison of severity of aortic regurgitation by cardiovascular magnetic resonance versus transthoracic echocardiography. Am J Cardiol 2011;108:1014-20.
84. Myerson SG, d'Arcy J, Mohiaddin R, et al. Aortic regurgitation quantification using cardiovascular magnetic resonance: association with clinical outcome. Circulation 2012;126:1452-60.
85. Lang RM, Bierig M, Devereux RB, et al. Recommendations for chamber quantification. Eur J Echocardiogr 2006;7:79-108.
86. Lang RM, Badano LP, Tsang W, et al. EAE/ASE recommendations for image acquisition and display using three-dimensional echocardiography. Eur Heart J Cardiovasc Imaging 2012;13:1-46.
87. Teichholz LE, Kreulen T, Herman MV, Gorlin R. Problems in echocardiographic volume determinations: echocardiographic-angiographic correlations in the presence of absence of asynergy. Am J Cardiol 1976;37:7-11.
88. Soliman OI, Kirschbaum SW, van Dalen BM, et al. Accuracy and reproducibility of quantitation of left ventricular function by real-time three-dimensional echocardiography versus cardiac magnetic resonance. Am J Cardiol 2008;102:778-83.
89. Hansegard J, Urheim S, Lunde K, Malm S, Rabben SI. Semi-automated quantification of left ventricular volumes and ejection fraction by real-time three-dimensional echocardiography. Cardiovasc Ultrasound 2009;7:18.
90. Kilner PJ, Gatehouse PD, Firmin DN. Flow measurement by magnetic resonance: a unique asset worth optimising. J Cardiovasc Magn Reson 2007;9:723-8.
91. Kramer CM, Barkhausen J, Flamm SD, Kim RJ, Nagel E. Standardized cardiovascular magnetic resonance (CMR) protocols 2013 update. J Cardiovasc Magn Reson 2013;15:91.
92. Buonocore MH, Bogren H. Factors influencing the accuracy and precision of velocity-encoded phase imaging. Magn Reson Med 1992;26:141-54.
93. Jehenson P, Westphal M, Schuff N. Analytical method for the compensation of eddy-current effects induced by pulsed magnetic field gradients in NMR systems. Journal of Magnetic Resonance 1990;90:264-278.
94. Van Vaals JJ, Bergman AH. Optimization of eddy-current compensation. Journal of Magnetic Resonance 1990;90:52-70.
95. Bernstein MA, Zhou XJ, Polzin JA, et al. Concomitant gradient terms in phase contrast MR: analysis and correction. Magn Reson Med 1998;39:300-8.
96. Rolf MP, Hofman MB, Gatehouse PD, et al. Sequence optimization to reduce velocity offsets in cardiovascular magnetic resonance

volume flow quantification - a multi-vendor study. J Cardiovasc Magn Reson 2011;13:18.
97. Alfakih K, Plein S, Thiele H, Jones T, Ridgway JP, Sivananthan MU. Normal human left and right ventricular dimensions for MRI as assessed by turbo gradient echo and steady-state free precession imaging sequences. J Magn Reson Imaging 2003;17:323-9.
98. Lotz J, Meier C, Leppert A, Galanski M. Cardiovascular flow measurement with phase-contrast MR imaging: basic facts and implementation. Radiographics 2002;22:651-71.
99. Bland JM, Altman DG. Statistical methods for assessing agreement between two methods of clinical measurement. Lancet 1986;1:307-10.
100. Altman DG, Bland JM. Diagnostic tests 3: receiver operating characteristic plots. BMJ 1994;309:188.
101. Altman DG, Bland JM. Diagnostic tests. 1: Sensitivity and specificity. BMJ 1994;308:1552.
102. Deeks JJ, Altman DG. Diagnostic tests 4: likelihood ratios. BMJ 2004;329:168-9.
103. Bland JM, Altman DG. Measuring agreement in method comparison studies. Stat Methods Med Res 1999;8:135-60.
104. Uretsky S, Supariwala A, Nidadovolu P, et al. Quantification of left ventricular remodeling in response to isolated aortic or mitral regurgitation. J Cardiovasc Magn Reson 2010;12:32.
105. Lang RM, Badano LP, Mor-Avi V, et al. Recommendations for cardiac chamber quantification by echocardiography in adults: an update from the American Society of Echocardiography and the European Association of Cardiovascular Imaging. Eur Heart J Cardiovasc Imaging 2015;16:233-70.
106. Polte CL, Lagerstrand KM, Gao SA, Lamm CR, Bech-Hanssen O. Quantification of Left Ventricular Linear, Areal and Volumetric Dimensions: A Phantom and in Vivo Comparison of 2-D and Real-Time 3-D Echocardiography with Cardiovascular Magnetic Resonance. Ultrasound Med Biol 2015.
107. Bushberg JT, Seibert JA, Leidholdt EM, Jr,, Boone JM. Ultrasound. In: The essential physics of medical imaging. Philadelphia: Lippincott Williams & Wilkins, 2012a:500-576.
108. Kremkau FW. Diagnostic ultrasound: principles and instrumentation. 7th ed: Saunders, 2006.
109. Hedrick WR, Hykes DL, Starchman DE. Ultrasound physics and instrumentation. 4th ed: Elsevier, 2005.
110. Bushberg JT, Seibert JA, Leidholdt EM, Jr,, Boone JM. Magnetic resonance imaging. In: The essential physics of medical imaging. Philadelphia: Lippincott Williams & Wilkins, 2012b:449-499.
111. Brown RW, Cheng YN, Haacke EM, Thompson MR, Venkatesan R. Magnetic resonance imaging: physical principles and sequence design. 2nd ed: Wiley Publishing, 2014.

112. McRobbie DW, Moore EA, Graves MJ, Prince MR. MRI: from picture to proton. 2nd ed: Cambridge University Press, 2007.
113. Westbrook C, Roth KR, Talbot J. MRI in practice. 3rd ed: Blackwell Publishing, 2005.
114. Jenkins C, Moir S, Chan J, Rakhit D, Haluska B, Marwick TH. Left ventricular volume measurement with echocardiography: a comparison of left ventricular opacification, three-dimensional echocardiography, or both with magnetic resonance imaging. Eur Heart J 2009;30:98-106.
115. Turner SP, Monaghan MJ. Tissue harmonic imaging for standard left ventricular measurements: fundamentally flawed? Eur J Echocardiogr 2006;7:9-15.
116. Rabben SI. Technical principles of transthoracic three-dimensional echocardiography. In: Badano LP, Lang RM, Zamorano JL, eds. Textbook of real-time three dimensionsal echocardiography. London: Springer, 2011:9-24.
117. Barkhausen J, Ruehm SG, Goyen M, Buck T, Laub G, Debatin JF. MR evaluation of ventricular function: true fast imaging with steady-state precession versus fast low-angle shot cine MR imaging: feasibility study. Radiology 2001;219:264-9.
118. Moon JC, Lorenz CH, Francis JM, Smith GC, Pennell DJ. Breath-hold FLASH and FISP cardiovascular MR imaging: left ventricular volume differences and reproducibility. Radiology 2002;223:789-97.
119. Senior R, Andersson O, Caidahl K, et al. Enhanced left ventricular endocardial border delineation with an intravenous injection of SonoVue, a new echocardiographic contrast agent: A European multicenter study. Echocardiography 2000;17:705-11.
120. Moceri P, Doyen D, Bertora D, Cerboni P, Ferrari E, Gibelin P. Real time three-dimensional echocardiographic assessment of left ventricular function in heart failure patients: underestimation of left ventricular volume increases with the degree of dilatation. Echocardiography 2012;29:970-7.
121. Chuang ML, Gona P, Hautvast GL, et al. Correlation of trabeculae and papillary muscles with clinical and cardiac characteristics and impact on CMR measures of LV anatomy and function. JACC Cardiovasc Imaging 2012;5:1115-23.
122. Papavassiliu T, Kuhl HP, Schroder M, et al. Effect of endocardial trabeculae on left ventricular measurements and measurement reproducibility at cardiovascular MR imaging. Radiology 2005;236:57-64.
123. Kondo C, Caputo GR, Semelka R, Foster E, Shimakawa A, Higgins CB. Right and left ventricular stroke volume measurements with velocity-encoded cine MR imaging: in vitro and in vivo validation. AJR Am J Roentgenol 1991;157:9-16.
124. Globits S, Pacher R, Frank H, et al. Comparative assessment of right ventricular volumes and ejection fraction by thermodilution and

magnetic resonance imaging in dilated cardiomyopathy. Cardiology 1995;86:67-72.
125. Chai P, Mohiaddin R. How we perform cardiovascular magnetic resonance flow assessment using phase-contrast velocity mapping. J Cardiovasc Magn Reson 2005;7:705-16.
126. Chatzimavroudis GP, Walker PG, Oshinski JN, Franch RH, Pettigrew RI, Yoganathan AP. Slice location dependence of aortic regurgitation measurements with MR phase velocity mapping. Magn Reson Med 1997;37:545-51.
127. Kozerke S, Schwitter J, Pedersen EM, Boesiger P. Aortic and mitral regurgitation: quantification using moving slice velocity mapping. J Magn Reson Imaging 2001;14:106-12.
128. Cawley PJ, Hamilton-Craig C, Owens DS, et al. Prospective comparison of valve regurgitation quantitation by cardiac magnetic resonance imaging and transthoracic echocardiography. Circ Cardiovasc Imaging 2013;6:48-57.
129. Uretsky S, Gillam L, Lang R, et al. Discordance between echocardiography and MRI in the assessment of mitral regurgitation severity: a prospective multicenter trial. J Am Coll Cardiol 2015;65:1078-88.
130. Polte CL, Bech-Hanssen O, Johnsson AA, Gao SA, Lagerstrand KM. Mitral regurgitation quantification by cardiovascular magnetic resonance: a comparison of indirect quantification methods. Int J Cardiovasc Imaging 2015.
131. Muzzarelli S, Monney P, O'Brien K, et al. Quantification of aortic flow by phase-contrast magnetic resonance in patients with bicuspid aortic valve. Eur Heart J Cardiovasc Imaging 2014;15:77-84.
132. Burris NS, Hope MD. Bicuspid Valve-Related Aortic Disease: Flow Assessment with Conventional Phase-Contrast MRI. Acad Radiol 2015.
133. Hope MD, Hope TA, Meadows AK, et al. Bicuspid aortic valve: four-dimensional MR evaluation of ascending aortic systolic flow patterns. Radiology 2010;255:53-61.
134. Hope TA, Markl M, Wigstrom L, Alley MT, Miller DC, Herfkens RJ. Comparison of flow patterns in ascending aortic aneurysms and volunteers using four-dimensional magnetic resonance velocity mapping. J Magn Reson Imaging 2007;26:1471-9.